

**DEVELOPMENT OF A NON-INDUCTIVE HIGH VOLTAGE D-DOT PROBE VOLTAGE TRANSDUCER SYSTEM**

*(PEMBINAAN SISTEM TRANSDUSER VOLTAN TINGGI TIDAK BERINDUKTIF BERASASKAN PROB D-DOT )*

**ZULKURNAIN B. ABDUL MALEK**

**RESEARCH VOTE NO:  
71598**

**Institut Voltan & Arus Tinggi  
Fakulti Kejuruteraan Elektrik  
Universiti Teknologi Malaysia**

**2003**

## **Acknowledgement**

*The author would like to acknowledge and thank The Research & Management Centre, Universiti Teknologi Malaysia for providing the grant for this research.*

## Abstract

Since the introduction of zinc-oxide material in 1968 much research has been directed towards the characterisation of the electrical behaviour of the material under various stress conditions. There is now an extensive published literature on the response of the material to impulse current stresses of different shape and amplitude. An aim of some of these investigations is to achieve an equivalent circuit representation which adequately simulate the observed test results. An adequate equivalent circuit representation will aid the reliable and efficient design of the overvoltage protection and help to improve the optimisation of the protective devices.

A significant impediment to the accurate characterisation of zinc oxide has been the lack of reliable test data especially for fast-rate-of-rise impulses in the microsecond and sub-microsecond range. The measurement of residual voltages using impulses in this range is highly influenced by the circuit arrangement and measurement transducer characteristics.

The measurement of voltage using parallel connected transducers is inherently affected by circuit inductances and the transfer characteristic of the divider itself. An improved voltage transducer based upon the D-dot probe principle was adopted. Previous published results obtained using this transducer showed that there is no evidence to link the voltage overshoot seen on the residual voltage trace of zinc oxide with the characteristics of the material itself. This observation has positive implications for the protective performance of zinc oxide and will allow a more accurate characterisation of the material.

## Abstrak

Sejak 1968 iaitu apabila bahan zink oksida mula digunakan, banyak penyelidikan telah dilaksanakan dan ianya tertumpu kepada pencirian elektrik bahan tersebut dalam pelbagai keadaan tegasan. Sekarang terdapat banyak kajian literatur yang terkumpul berkenaan tindakbalas bahan zink oksida terhadap dedenyut arus pelbagai bentuk dan amplitud. Tujuan utama kajian yang dilaksanakan ialah untuk mendapatkan perwakilan litar setara zink oksida. Perwakilan litar setara yang sesuai dapat membantu dalam penghasilan rekabentuk perlindungan voltan lampau yang mempunyai keboleharapan dan kecekapan yang tinggi dan juga membantu penggunaan peralatan perlindungan secara optimum.

Satu penghalang penting untuk pencirian zink oksida secara tepat ialah kurangnya data ujikaji terutamanya untuk dedenyut yang mempunyai kadar menaik yang pantas dan dalam julat sub-mikro saat hingga mikro saat. Pengukuran voltan baki menggunakan dedenyut dalam julat ini sangat dipengaruhi oleh susunatur litar dan ciri-ciri transduser.

Pengukuran voltan menggunakan transduser yang disambung selari dipengaruhi oleh keruhan litar dan ciri-ciri pemindahan pembahagi voltan tersebut. Dalam kajian ini, transduser voltan berasaskan prinsip prob D-dot digunakan. Data dari kajian terdahulu menunjukkan tiada kaitan di antara lajukan pada voltan baki zink oksida dengan ciri-ciri bahan zink oksida. Pemerhatian ini mempunyai kesan positif kepada prestasi perlindungan zink oksida dan pencirian bahan zink oksida yang lebih tepat dapat dicapai.

## CONTENTS

<b>TOPICS</b>	<b>PAGE</b>
Acknowledgement	ii
Abstract	iii
Abstrak	iv
Contents	v
List of Table	viii
List of Figure	ix

### **CHAPTER 1            INTRODUCTION**

1.1	Background	1
1.2	Objectives	3
1.3	Scope of Project	4
1.4	Direction of Project	4
1.5	Expected Results/Benefits	4

### **CHAPTER 2            IMPROVED**

2.1	Introduction	5
2.2	Review	8
2.2.1	Previous Techniques and Errors	9
2.2.1.1	Voltage Measurements with Dividers	9
2.2.1.2	Parallel Measurement	12
2.2.1.3	Coaxial Measurements	12

2.3	New Technique	13
2.3.1	Objectives	13
2.3.2	Principles of The Series Voltage Divider	13
2.3.3	Practical Arrangement	14
2.3.4	A D-Dot Based Sensor	17

### **CHAPTER 3            D-DOT PROBE BASED SENSOR**

3.1	Introduction	19
3.2	Theory and Equivalent Circuit	19
3.3	Probe Description and Design Criteria	21
3.4	Computer Simulation of the Probe	23
3.4.1	SLIM: Electromagnetic Engineering	23
3.4.2	Determination of the Maximum Electric Field	24
3.4.3	Effect of Shielding/Field Modifying Toroids	27
3.4.4	Calculation of the Probe Ratio	27

### **CHAPTER 4            D-DOT PROBE DESIGN**

4.1	Materials	34
4.1.1	Aluminium	34
4.2	Physical Structure	37
4.2.1	Coaxial Arrangement	37
4.2.2	Hollow (expand) Conductors	37
4.3	System Characteristic Parameters	38
4.3.1	Skin Effect	38
4.3.2	Corona Effect	38
4.3.3	Conductor Losses	39
4.4	Complete Design	40
4.4.1	Materials for D-dot Probe	40
4.4.2	Engineering Drawing	40

**CHAPTER 5 CONCLUSION AND SUGGESTIONS**

5.1	Discussion	53
5.2	Conclusions	55
5.3	Suggestions	56

<b>REFERENCES</b>	<b>57</b>
-------------------	-----------

**LIST OF TABLE**

<b>TABLE NO.</b>	<b>TOPIC</b>	<b>PAGE</b>
Table 4.1	Materials used for D-dot Probe Assembly	41



**LIST OF FIGURES**

<b>FIGURE NO.</b>	<b>TOPIC</b>	<b>PAGE</b>
2.1	Typical test arrangement for impulse testing of ZnO surge arresters.	12
2.2	Schematic diagram of ZnO test object-series divider-current shunt arrangement.	16
3.1	Theory of the probe.	20
3.2	Equivalent Circuit of The Probe.	20
3.3	Schematic of the D-dot probe assembly	22
3.4	2D Mesh Generation.	25
3.5	Vector Display (Scaled Mode).	25
3.6	D-Dot probe equipotential contours at intervals of 1per-unit.	26
3.7	Electric Field Along High Voltage Rod.	26
3.8	Definition of the probe capacitances.	28
3.9	2D Mesh Generation.	29

3.10	Vector Display (Color Mode).	29
3.11	Vector Display (Scaled Mode).	29
3.12	D-Dot probe equipotential contours at intervals of 1 per-unit.	30
3.13	Flux Density Over the Surface of The High Voltage Conductor.	30
3.14	Electric Field Over the Surface of The High Voltage Conductor	31
3.15	Flux Density Over the Surface of The High Voltage conductor	31
3.16	Electric Field Over the Surface of The High Voltage Conductor	32
3.17	Voltage potential at signal toroid versus distance.	32
4.1	Component in the D-dot probe.	42
4.2	D-dot probe view from one side.	42
4.3	Dimension of D-dot probe (slice at the middle).	43
4.4	Dimension of D-dot probe with attenuator.	43
4.5	Schematic diagram of D-dot probe arrangement.	44
4.6	Perspex support for high voltage rod.	44

4.7	Perspex support for high voltage rod (3 D view).	45
4.8	High voltage rod without ending screw	45
4.9	High voltage rod without ending screw (3 D view).	46
4.10	Solid ending screw for high voltage rod.	46
4.11	Solid ending screw for high voltage rod (3 D view).	47
4.12	Signal and grounding toroids.	47
4.13	Stress modifying toroids.	48
4.14	Thin cylinder aluminium. (inner).	48
4.15	Thin cylinder aluminium, (outer).	49
4.16	Attenuator.	50
4.17	Attenuator (3 D view).	51
4.18	Attenuator schematic arrangement.	52
4.19	Attenuator arrangement.	53

**LIST OF SYMBOLS**

DC,dc	-	Direct current
Ac,ac	-	Alternating current
Hz	-	Hertz
C	-	Capacitance
D	-	Electric flux density
E	-	Electric field Intensity
F	-	Farad
R	-	Resistance
D		Diameter
Q,q	-	Charge
f	-	Frequency
ZnO	-	Zinc Oxide
I,i	-	Current
V,v	-	Potential difference

$\varepsilon$	-	Permittivity
$\delta$	-	Distance
$\alpha$	-	Angle
$r$	-	Radius
$t$	-	Time
$h$	-	Distance, length
$\rho_1$	-	Line charge density
$\omega$	-	Radian frequency
$\tau$	-	Transit time
mm	-	Millimeter
m	-	Meter

## CHAPTER I

### INTRODUCTION

#### 1.1 Introduction

Waveform measurements of rapidly changing voltages and currents give rise to special difficulties in high-voltage technology. Because crest values may reach several million volts or amperes, direct measurement is impractical and scaling of the original signal to smaller values produces a reduced signal  $V_m(t)$ , which is approximately proportional to the quantity to be measured into the signal  $V_m(t)$ , as well as its transmission and display, is subject to inherent system errors. In addition, electromagnetic fields associated with rapidly changing phenomena induce disturbance voltages in the measuring circuit so that arrangements that are satisfactory for most electronic test may not be applicable [1].

The measurement of voltage and current in high voltage tests is difficult because amplitudes are so high that they cannot be measured directly with conventional measuring and recording systems. Furthermore, not only the peak value but also the shape of the measured signal should be measured and

evaluated, particularly for impulse voltage and current, and this requires an adequate recording system using either an oscilloscope or a digital recorder.

Accurate high voltage measurements are required by the electric power industry for instrumentation, metering, and testing applications. Similarly, there is a need for accurate measurements of high voltages in pulsed power machines to monitor and optimize machine operation. The accurate measurement of fast transient voltages is also important in the assessment of their effects on electrical power equipment and insulation in order to improve system reliability. Additionally, for the correct evaluation of transient voltage effects on apparatus or dielectrics, the peak voltage and wave shape must be accurately known.

Steady-state high voltages can be measured with much smaller uncertainties than high-voltage transients can be. For example, calibrations of dc high-voltage dividers for divider ratio have been routinely performed in the range of 10 kV to 100 kV with relative uncertainties of less than 0.01 %. AC divider ratios have been calibrated over the same voltage range with 0.05 % relative uncertainties. High voltage impulses, on the other hand, are much more difficult to measure accurately because of the wide-bandwidth devices and instrumentation necessary to faithfully capture the high-frequency components of these transient signals. Typically, the measurement devices used for scaling the voltages to measurable levels must be physically large to be capable of withstanding the high voltages imposed on them and their large size makes them susceptible to wave propagation effects, pickup of extraneous signals, stray capacitance, and residual inductance effects that distort the measurements of fast transients.

Recently, international standards on high-voltage test techniques have been introduced that require voltage dividers used in high-voltage impulse measurements to be traceable to national standards. A facility for the testing of pulse voltage dividers has been developed in response to the needs of the electric power and the pulsed power communities. The divider itself must have

adequate insulation and physical dimensions large enough to with-stand the full applied voltage, but must also have the wide bandwidth necessary to scale microsecond or submicrosecond high-voltage transients with minimal distortion. Additionally, the voltage recorder must have sufficient resolution to measure the fast waveforms.

## 1.2 Objectives

The main aim of this project is to develop and build a high voltage impulse voltage measuring system suitable for zinc oxide surge arrester fast transient studies. The design is based on the D-Dot probe capacitive divider, which is used for non-inductive residual voltage measurements across zinc oxide surge arresters. To achieve this the objectives of this project are therefore:

1. to obtain the engineering drawing using the AutoCAD drawing package;
2. to get the best configuration and arrangement of the probe design using the SLIM package;
3. to determine the field configuration of the probe;
5. to compute the probe capacitance and the low voltage arm capacitance;
6. to understanding the physical structure of the D-Dot probe;
7. to directly compare the efficiency of the D-Dot probe with other high voltage dividers.



### **1.3 Scope**

The work involves the design and construction of a fast impulse measuring system based on the D-dot probe principle. The impulse voltage transducer will be incorporated in a later project on the design and construction of a 100 kV coaxial test module.

### **1.4 Direction of the Project**

The direction of the present work is to design better techniques for measure non-inductive impulse voltage for ZnO surge arrester. So, in this project, the characteristic of impulse voltage, ZnO surge arrester, voltage divider principle and lastly a new designed D-Dot probe based sensor will discussed for voltage measurement. This work was suggested by a method of voltage measurement on specially adapted ZnO surge arresters in service

In this project, the above method is adapted to measure very fast transients in standard arresters and to avoid the effects of stray inductances.

### **1.5 Expected Results/Benefits**

A new voltage transducer system suitable for fast transient response measurements complete with signal capturing facilities. This transducer will be incorporated in the 100 kV low inductance test module for zinc oxide fast transient studies. Ultimately, a new set of zinc oxide characterisation based on the test results obtained using the test module will be achieved.

## **CHAPTER II**

### **IMPROVED IMPULSE VOLTAGE MEASUREMENT TECHNIQUES**

#### **2.1 Introduction**

Over the last two decades, ZnO surge arresters have gained a widespread recognition of their superior performance compared to SiC arresters and other conventional overvoltage protection devices [2]. Among the numerous advantages of ZnO arresters are highly non-linear voltage characteristics, better energy absorption, elimination of power frequency follow current and lower protective levels. The most significant advantage however is the fast switching of the arrester from a nearly open circuit at power frequency working (system) voltage to very low resistance during the period of the overvoltage. This offers the possibility of an adequate means of protection for most overvoltages especially very fast front transient overvoltages such as those generated in modern GIS.

Much research work has been published on the fast transient performance of ZnO arresters. Most of these tests showed an initial spike/overshoot on the measured residual voltages waveforms. Extensive

studies of this unexplained phenomenon suggested that the initial voltage overshoot is affected by the circuit inductance and coupling, impulse rate of rise, the impulse amplitude, the nature and amount of additives, the pre-injection of carriers, the value of the non-linearity coefficient and the difference in the rate of charge accumulation at the electron and hole traps located at the interface of the grain and intergranular layer. In contrast, some of these investigations emphasized that this overshoot is not observable when testing SiC material, which implied an association of the overshoot with ZnO material fast switching capabilities and suggestions that it takes a significant time for ZnO material to turn-on resulting in a delay in switching from a high to low resistance state [2].

This time to turn-on however, is not conclusively established. Very fast transient (less than 500ps) test [3] on small ZnO varistors showed that the material did not exhibit any measurable time delay in the transition to high conduction for that particular small-scale arrangement. On the other hand, high voltage tests indicated that it takes up to 3ns for ZnO to switch from capacitive to resistive behaviour. One difference between small and large-scale experiments is the size of the circuits loops, which could influence any inductive effects as will explained in the next section.

In practical applications of surge arresters, the presence of a significant overshoot in the transient voltage across the device protected by the arrester could be damaging. It is important to identify the nature of this overshoot. That part of the overshoot, which is inherent in the arrester, with its non-linear ZnO elements, housing and terminations, is unavoidable. However, in test procedures, other sources of overshoot may be more significant:

- a) The inductance of the test voltage source and its connections to the arrester may, in combination with the relatively large capacitance associated with the high permittivity ZnO elements, cause an initial voltage overshoot at the arrester terminals.

- b) High-voltage measurements are usually made with parallel-connected voltage dividers. The transfer characteristics of parallel-connected dividers are determined by the inherent inductive and capacitive effects associated with both the high and low-voltage arms of the divider, which can limit the response time and cause a voltage overshoot at the high-voltage terminal and/or the signal output to the recorder.
  
- c) The test circuit arrangement can also be important. If the voltage-divider connection to the arrester also carries the discharge current of the arrester, inductive effects are clearly greater. In the application of surge arresters to cable and transformer protection in power systems, this source voltage overshoot (distance effect) is unavoidable but can be minimized by situating the arrester as close as possible to the protected unit.

By applying suitable techniques, it is possible to minimize the above sources of overshoot. Voltage measurements with such circuits are obviously influenced by the current rate of rise, its amplitude and the physical size of the loops which determine both the self-inductances and mutual inductance between the current and measuring loops.

In this chapter, conventional voltage measurement techniques will first be discussed in order to understand the significance of the measurement and its relation to the properties of ZnO material. Then a new method of improved voltage measurement technique will be described and explained which minimize the effects discussed in points a) to c).

## 2.2 Review

Nowadays impulse voltage measurements are performed with resistive or capacitive voltage dividers. The main duties of a precise voltage measurement with voltage dividers are discussed. It will be shown that every high voltage divider has a limitation for the measurement of front oscillations or front-chopped lightning impulse voltages. On the other hand a voltage divider can be easily calibrated and can be constructed to prevent EMC-problems during impulse voltage measurement.

With the development of an electric field sensor with optoelectronic data transmission, a voltage measurement system is now available with an upper bandwidth of 25 MHz. The essential advantage is the distortion-free measurement of all impulse test voltages in any circuit. After a short review of the principle and characteristics of the new developed sensor, some practical applications will be dealt with. It will be shown that the new sensor can improve the high voltage measurement [4].

The measurement of high voltages in laboratories or power systems is performed with capacitive, inductive or resistive dividers or with a combination of components of these. The duty of the voltage divider is to reduce the high voltage of some million volts to a voltage of some 100 volts. This low voltage should be an image of the high voltage only reduced by a constant factor, the ratio. The ratio should therefore be independent of e.g. the amplitude of the applied voltage, the temperature, the frequency, the surrounding etc. then this low voltage can be indicated by an instrument.

Recent developments in fiberoptic transmission systems have resulted in a measuring system with an electric field sensor, applied now to high voltage impulse measurement. It is the aim of this project to discuss at first

the main problems in high voltage impulse measurement with voltage dividers and to show the theoretical limitation of this kind of apparatus. Afterwards the new sensor will be presented and the limitation of this system will be discussed. The last part should show some practical applications and an idea how high voltage-measuring systems can be designed.

## **2.2.1 Previous Techniques and Errors**

### **2.2.1.1 Voltage Measurement with Dividers**

Practically in all application of high voltage measurement, the used principle is the voltage divider. Two basic circuits, the resistive voltage divider and the capacitive voltage divider are applied. The high voltage of some millions of volts is reduced to a level of some 100 volts.

The influence of the impedance of a voltage divider on the generation circuit cannot be neglected. Therefore this impedance has to be dimensioned not only according to the measuring requirements for high impulse voltages but also to the load requirements of the circuit.

The frequency limitation of the resistive voltage divider is given by the value of the high voltage resistance  $R_1$ . The upper limit of the bandwidth of this voltage divider is proportional to the reciprocal value of the time constant given by  $R_1$  and the earth capacitance  $C_e$ . On the other hand the time to half value  $T_2$  of any impulse voltage is proportional to  $R_p \cdot C_s$ , with  $C_s$  the impulse capacitance of the generator and  $R_p$  the total parallel resistance of the circuit.

A high bandwidth of the measuring device asks for a small resistance  $R_1$ . On the other hand the resistance  $R_p$ , including  $R_1$  has to be increased for longer times to half value, e.g. for switching impulse voltages. Hence the resistive voltage divider can only be applied to the measurement of lightning impulse voltages up to about 2 MV.

The ratio of the capacitive voltage divider is influenced by the earth capacitance. The higher the capacitance  $C_1$  of the divider the smaller is the influence of the earth capacitance  $C_{eff}$  of a voltage measuring system, given by  $C_1$  and  $C_e$  increases the load capacitance of the generating circuit. Therefore this capacitance  $C_{eff}$  limits the maximum load capacitance acceptable for a given circuit to generate the lightning impulse voltage with a front time  $T_1$  within the range given by the standards. The second problem of the capacitive voltage divider is the limited bandwidth. Because of the resonance frequency of the measuring circuit given by the inductance of the lead and the effective capacitance of the divider an oscillation occurs in the measurement of lightning impulse voltages. For the measurement of switching impulse and a.c. voltages up to the highest values the only critical point in the application of the capacitive voltage divider is the influence of the earth capacitance on the accuracy of the ratio. This can be taken into account by an adequate calibration procedure.

In the testing technique two cases are well known resulting in higher frequencies than some MHz. The first one is front oscillations in lightning impulse voltages, excited by the firing of a multistage impulse generator and caused by the reflections at the load capacitance. These front oscillations occur at about 10 to 40% of the impulse amplitude and can increase the difficulty in the evaluation of the correct front time (30%-point). The front oscillations are more pronounced with increasing number of stages of an impulse generator, and the frequency is reduced with increasing circuit dimensions.

Resulting in higher frequencies than some MHz, is the measurement of chopped lightning impulse voltages. Depending on the chopping device and the test circuit, frequencies of some 10 MHz are possible. In the test technique the exact shape of the voltage collapse is not of interest, but the amplitude of the test voltage and the time to chopping should be measured accurately. Because of the limited bandwidth of each voltage divider and because of the arrangement of the measuring circuit two problems can be realized. The limited transfer characteristic results in the measurement of a too low voltage amplitude (theoretical this error can be corrected with the response time). Additionally the electromagnetic field traveling directly to the lower part of the voltage divider influences the measured signal, resulting in some disturbances at the beginning of the chopping.

The most important part of a voltage divider for measuring purposes is the low voltage arm. The high voltage part has to be dimensioned according to circuit requirements, whereas the low voltage part can be optimized for the measurement. In this respect the low voltage arm should be constructed in a coaxial arrangement and earthed directly with impedance as low as possible. The low voltage should be chosen as high as possible. If all these points are taken into account, the low voltage part does not limit the voltage measurement. Additionally with different secondary units the low voltage can always be adapted in an optimal way. The calibration of the ratio of a divider is done by measuring the capacitance or resistances and the transfer characteristic is checked in the final circuit by the nit step method.

The voltage measuring device should measure the voltage at the test object or at another point of interest. To check the accuracy of the measurement and the applicability of the divider the transfer characteristics have to be measured in the final test arrangement. This point is often neglected in high voltage test laboratories during measurements.



### 2.2.1.2 Parallel Measurement

The residual voltage across a single ZnO element or complete arrester during the flow of discharge current is conventionally measured with a high voltage divider (capacitive or resistive or mixed type). The most important requirements of the divider are its transfer characteristic and response time.

Figure 2.1 shows a typical configuration for the direct measurement of residual voltage. Voltage measurements with such circuit are obviously influenced by the current rate of rise, its amplitude and the physical size of the loops which determine both the self inductance and mutual inductance between the current and measuring loops.

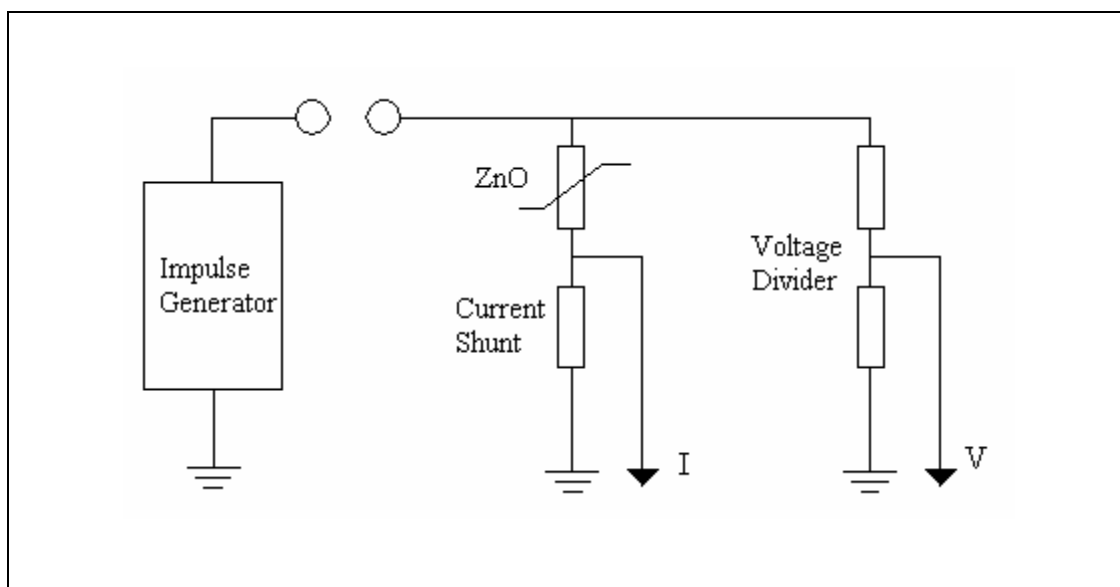


Figure 2.1 Typical test arrangement for impulse testing of ZnO surge arresters.

### **2.2.1.3 Coaxial Measurements**

In order to reduce mutual inductance effects, test measurements have been reported with ZnO samples having a central hole. The potential lead from the high-voltage terminal to the voltage divider is taken through the central hole which is free from magnetic field associated with the ZnO current so that no flux due to the this current can then link the measurement loop. The inductive effect can be reduced but some overshoot can still be seen if the system is not purely coaxial. Although a useful method, it is not suitable for complete arresters which do not contain a central hole [2].

## **2.3 New Technique**

### **2.3.1 Objectives**

It was demonstrated in the previous section that parallel voltage measurements could lead to unacceptable errors due to loop inductances and magnetic coupling of circuit loops. The solution proposed here to overcome this problem is fully compatible with complete ZnO arresters, is little affected by the induction process, and is suitable for measurements on both single elements and complete arresters.

### **2.3.2 Principle of the Series Voltage Divider**

The method obviates the use of a parallel connected voltage divider by using a thin ZnO slice/disc of the same materials as that of the test object

which is arranged in series at the bottom of the element/arrester to form a natural voltage divider with a ratio related to the disc thickness.

The concept of using a thin varistor disc has been independently proposed by Barker et al.[3]. Although not a coaxial arrangement, specially adapted arresters incorporated a thin element for field studies of arrester performance. In the present design of the series divider for use in laboratory test on standards arresters, the thin disc has a central hole to allow a coaxial pick up of the divided voltage. A low-voltage attenuator can then be located in a shielded box and will be unaffected by inductive effects.

Response time and transfer characteristic requirements on the low-voltage attenuator are easily met because of its smaller size and rating. However, the impedance of the attenuator should be much higher than that of the thin ZnO disc so that the current will flow through the ZnO disc and negligible error will be introduced by the presence of the attenuator in parallel with the disc.

### **2.3.3 Practical Arrangement**

Figure 2.2 shows the test arrangement [2]. The series divider (1) is connected between the ZnO element/arrester (2) and the cylinder conductor providing the current path to ground (3) or to a current shunt. A system of plane electrode (4a and 4b) is carefully designed to avoid local discharge and ensure uniformity of current through the thin disc. The potential lead (5) is connected to the upper electrode (4a) and brought to the central hole (6) of the ZnO thin disc. The lower electrode (4b), which is fixed to the current path

cylinder (3), also contains a central hole to allow the divider voltage to be applied to the attenuator (7).

The attenuator is enclosed in an aluminium cylinder (8) to provide double shielding and avoid adjacent current paths. The physical arrangement of the attenuator components inside the shielding cylinder (8) is designed to ensure coaxial flow of current and uniformity of stray components.

The low voltage signal output from the attenuator, is transferred to the digitizing oscilloscope via a 28m triaxial cable (9). The outer screen of the cable is isolated from the inner screen and it is connected to the current path cylinder. This ensures adequate screening against stray pick-ups and more importantly a fully coaxial measurement system similar to that used in tubular non-inductive current shunts.

The current path cylinder can then be earthed directly or via a resistance current shunt (10) if current measurement is necessary. No difference in the voltage signal was detected with the current shunt connected.

Although both inner and outer screens of the triaxial cable are earthed remotely in the measurement room, current signals are unaffected.

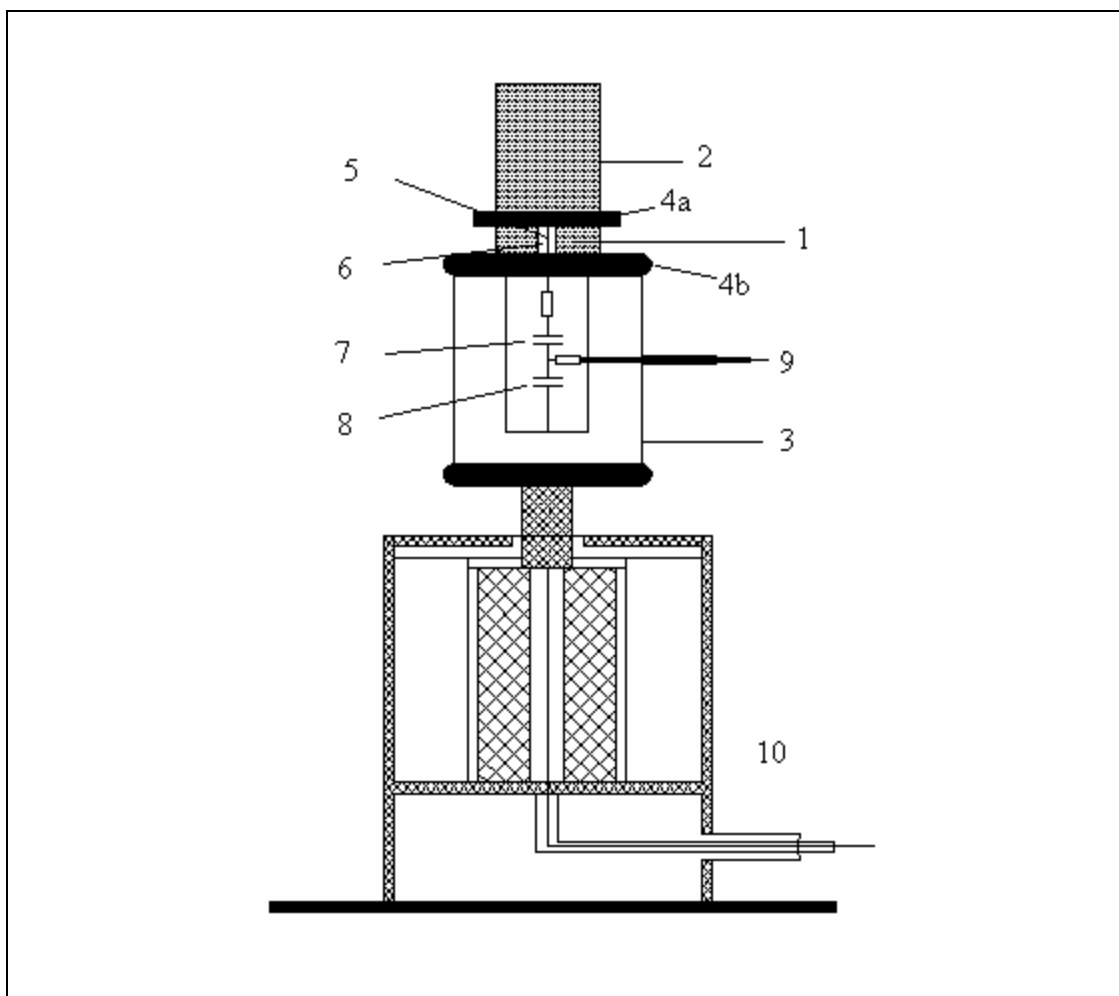


Figure 2.2 Schematic diagram of ZnO test object-series divider-current shunt arrangement.

1: series divider (thin disc), 2: ZnO arrester/element, 3: current path cylinder,  
 4a,b: plane electrodes, 5: potential lead, 6: central hole, 7: attenuator,  
 8: attenuator shielding cylinder, 9: triaxial cable, 10: tubular current shunt.

### 2.3.4 A D-Dot Probe Based Sensor

An alternative technique has been achieved using D-Dot (or capacitive) probe systems, which are a simple method of measuring transient voltages. By suitable choice of compensation and materials, frequency bandwidths from hertz to several tens of megahertz are achievable [5-7].

The probe essentially behaves as a capacitive divider. It is usually used in a coaxial configuration and takes the form of capacitance between the voltage carrying conductor and a voltage sensor, and a capacitance to ground (comprising capacitance to ground of the sensor, capacitance of the measuring cable, capacitance of measuring equipment and in addition if required an externally connected capacitor). The high voltage arm can thus be designed to be an integral structure within the test circuit and therefore to avoid the loop-inductance connection problems, which are inevitable with externally, connected dividers.

The d-dot probe was developed for the measurement of transient electric fields. For an electric field sensor the influence of the magnetic field component into the measuring circuit has to be negligible. To reach this goal, the screening of the electronic circuitry and the size and arrangement of the measuring and reference areas are important.

The main application of the sensor will be the voltage measurement in addition to the measurement with a divider. Special problems like front oscillations or the evaluation of front chopped impulse voltages can be solved with the new measuring device. Also the connection of the measuring device to the test object can be simpler and help to improve the test technique. For voltage measurement the sensor should be placed in vicinity to the high voltage electrode of the apparatus to be tested. With the distance of the probe

to the high voltage electrode the sensitivity of the measuring system can be influenced. The influence of other parts of the circuit on the measuring signal depends on the positioning of the sensor and determines the accuracy of the measurement. But if some simple precautions are fulfilled, the measurement of impulse voltages with the d-dot probe is easy to be performed. For special applications (mechanical stresses, electrostatic forces on the sensor or the electrodes) it can be necessary to fix the sensor rigidly to the electrode of interest.

In this project, the D-Dot probe based sensor is designed for non-inductive residual voltage measurements across zinc oxide surge arresters. The description of this design is discussed in the next chapter.

## **CHAPTER III**

### **D-DOT PROBE BASED SENSOR**

#### **3.1 Introduction**

D-Dot probes are field-coupled sensors, which are used to measure impulse voltages; they have attractive features including a non-intrusive installation, simplicity of construction and potentially wide bandwidth. Measurement of fast voltage transients by conventional dividers introduces inductive overshoots superimposed on the actual voltage waveforms. Moreover, this inductive effect slows the front of the waveform. In this project, complete design data (last part) are introduced for the new probe.

#### **3.2 Theory and Equivalent Circuit**

If it is desired to measure the voltage transients in a coaxial arrangement, where the axial rod is energized and the outer cylinder is earthed, and the inner core of a coaxial cable picks-up the voltage signal as



shown in Figure 3.1. The equivalent circuit can be given by the circuit shown in Figure 3.2., where  $C_1$  is the capacitance between the inner core and the axial high-voltage rod,  $C_2$  is the capacitance between the inner core and the port (at zero potential), and  $R_m$  is the matching resistance of the cable.

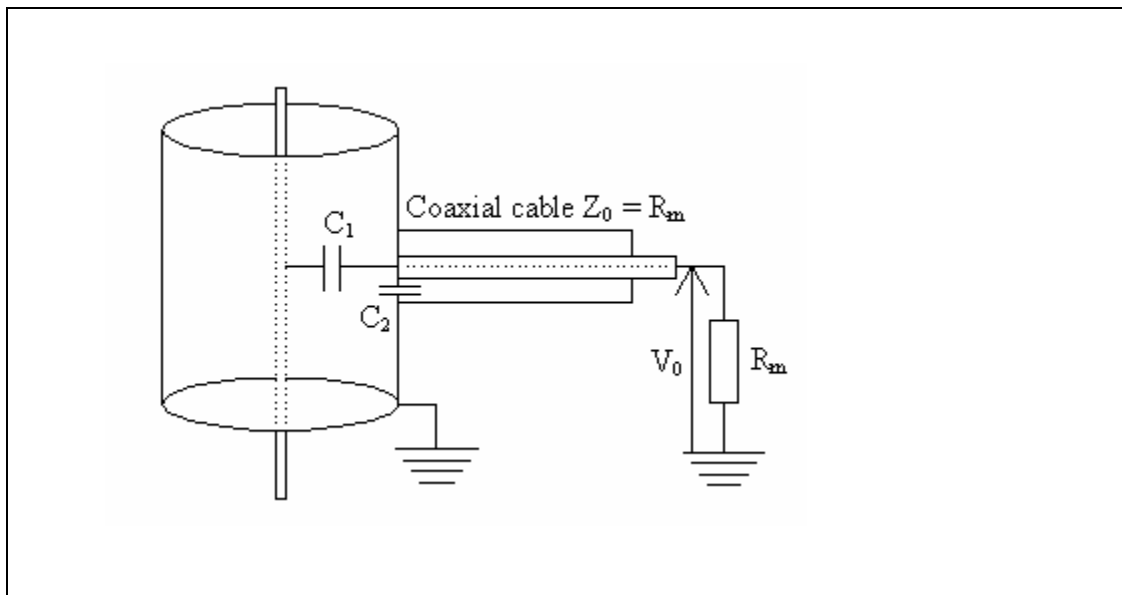


Figure 3.1: Theory of the probe.

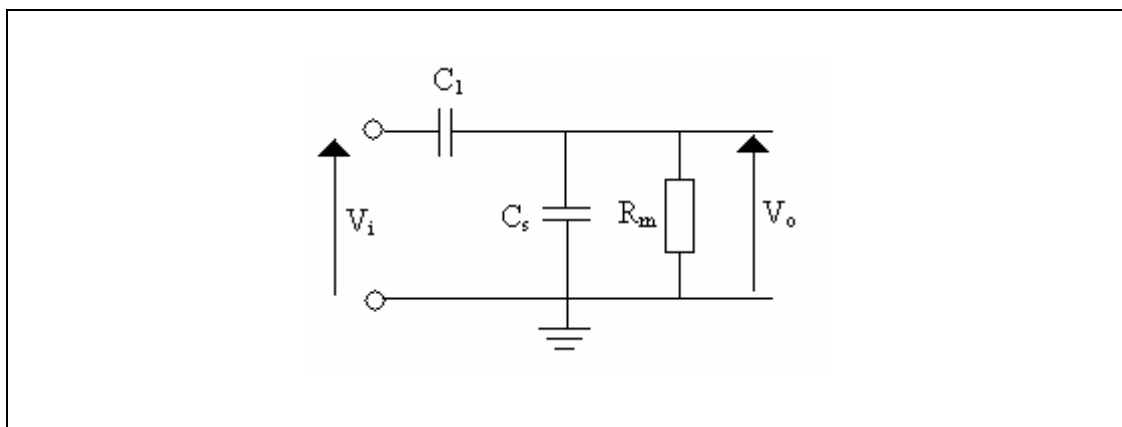


Figure 3.2:- Equivalent Circuit of The Probe

Normally  $C_2 \gg C_1$ , due to the physical size of the arrangement, and hence the equivalent circuit can be approximated to Figure 3.2, where the output voltage ( $V_0$ ) in the frequency domain is given by

$$V_0 = \frac{j\omega\tau}{1 + j\omega\tau}$$

where  $\tau = R_m C_1$ , and  $\tau$  is adjusted to be  $\gg \omega$ , then

$$V_0 = j\omega\tau V_i$$

### 3.3 Probe Description and Design Criteria

The D-Dot probe design proposed (Figure 3.3) essentially comprises three similar aluminium toroids (main outer diameter 407 mm, minor diameter 38 mm) placed coaxially around a cylindrical high voltage conductor. The three toroids are supported within a cylindrical aluminium tube. This facilitates easy removal and interchange of the probe to and from other test arrangements.

The outer toroids are equally spaced above and below a central sensor toroid. The outer toroids are electrically connected to ground and serve to shield the inner sensor toroid from extraneous fields/flux lines and provide a degree of field modification. The central toroid is electrically isolated from earth and forms the capacitance to the high voltage conductor. Two plates with rounded edges are fixed on the axial high-voltage rod to minimize the external electrostatic coupling with the toroid system and to reduce the maximum electric field along the axial rod. A means of connecting a coaxial signal cable (and if required an externally connected capacitor to ground) to the central toroid provided.

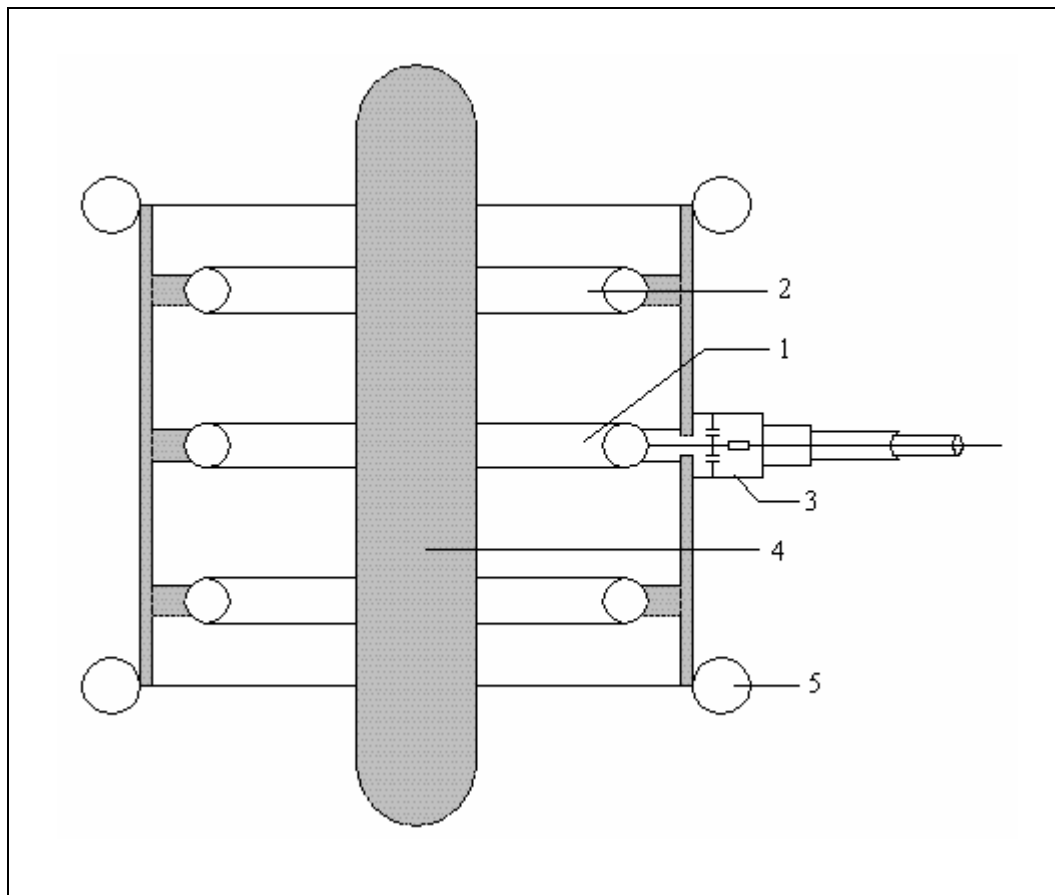


Figure3.3:- Schematic of the D-dot probe assembly

- 1: Signal toroid, 2: Grounded shielding toroids, 3: Low-voltage attenuator,  
4: High-voltage conductor, 5: Stress-modifying toroids.

The capacitance  $C_{hv}$  between the high voltage conductor and the central toroid forms the high voltage arm of the divider, and the stray capacitances between the toroid and ground  $C_g$ , the capacitance of the measuring cable  $C_c$  and the capacitance of the recording equipment  $C_r$  form the low voltage arm  $C_{lv}$ . An additional capacitor  $C_s$  connected in parallel with  $C_g$ ,  $C_c$  and  $C_r$  may be required to achieve the desired attenuation  $C_{hv}/(C_{lv} + C_{hv})$ .

One of the most important criteria in the design is to ensure that the highest local electric field at the maximum prospective arrester surge voltage of 50kV is of a sufficiently low value so as to ensure that neither partial

(corona) breakdown nor complete flashover will occur. An adequate safety factor is needed because the magnitude of the electric field which could give rise to partial or complete breakdown can be significantly lowered by the roughness of the conducting surfaces and by the accumulation of dust on those surfaces.

Secondly, any flux lines terminating on the signal toroid must originate only from the high voltage conductor and not, for example, from the test object. Finally the capacitance between the high voltage conductor and the signal toroid must be of sufficient value (very low) to provide an adequate signal ratio  $C_{hv}/(C_{lv} + C_{hv})$ . Due to mechanical consideration of the whole system the outer diameter of the toroids was fixed. Further modification in the capacitance value of the high voltage arm (once the diameter of the high voltage conductor was fixed) could be achieved by altering the spacing between the signal toroid and the shielding toroids. Increase of the spacing would tend to increase  $C_{hv}$  and decrease  $C_g$  and therefore  $C_{lv}$ .

### **3.4 Computer Simulation of the Probe**

#### **3.4.1 SLIM: Electromagnetic Engineering**

SLIM is a professionally engineered, fully integrated collection of software modules that provides facilities for the generation and solution of electromagnetic finite element models. SLIM has been continuously developed over the last 30 years by the ALSTOM Research & Technology Center and provides a state of the art design environment supported by professional engineers, mathematicians and computer scientists.

SLIM can improve product design and reduce development costs and has a satisfied customer base that includes major power transmission, distribution and generation companies, electrical machine manufacturers and R&D centers throughout the world. SLIM is the only electromagnetic finite element package that is commercially available from a manufacturer of electrical equipment and its development is driven by the requirements of experienced product designers.

#### **3.4.2 Determination of the Maximum Electric Field**

A lot of practical high voltage design requires knowing what the maximum E-field is, for insulation design, corona reduction, etc. The exact field can, of course, be calculated numerically by solving Laplace's equation over a suitable field with appropriate boundary conditions. As complicated and time consuming as this is, it is necessary when performance is critical, in integrated circuit design, designs for absolute minimum cost, and so forth. However, for more run of the mill experimentation and use, where a little overdesign can be tolerated, approximations to the field are just as useful.

In order to meet the above criteria computer modeling of the probe was conducted using a finite element program. The first consideration was to find a design, which would yield the lowest electrical field value (in particular at the point on the high voltage conductor adjacent to the signal toroid).

Simulation was necessary both to ensure that the electrical fields within the probe assembly were safely below the corona level at the maximum prospective voltage and to determine the optimum configuration for the desired probe capacitance. The effects of high voltage conductor profile and

spacing of the shielding toroids were investigated. The potentials contours for the final design configuration are shown in Figure 3.6.

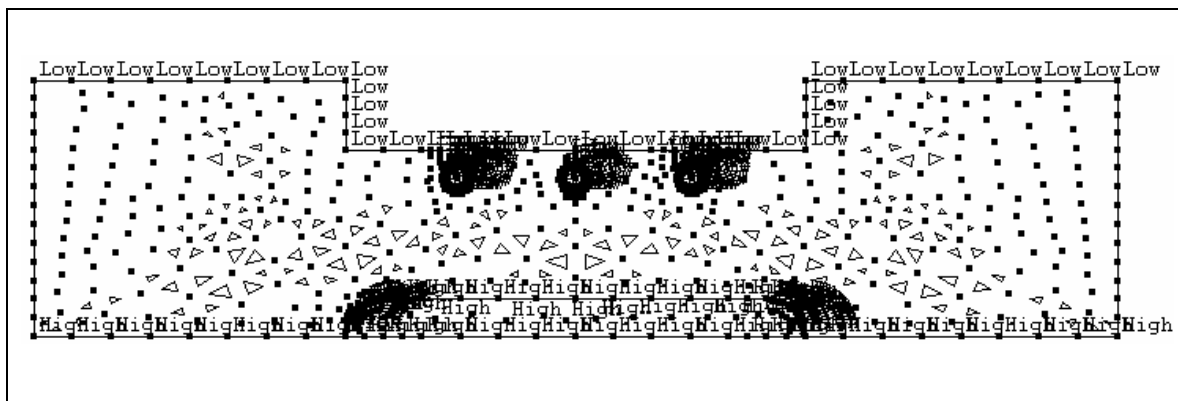


Figure 3.4:- 2D Mesh Generation

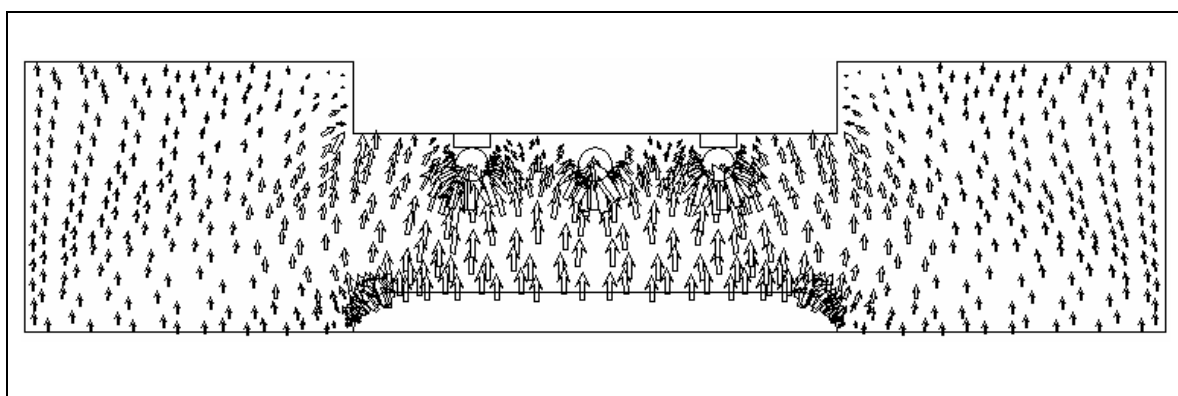


Figure 3.5:- Vector Display (Scaled Mode)

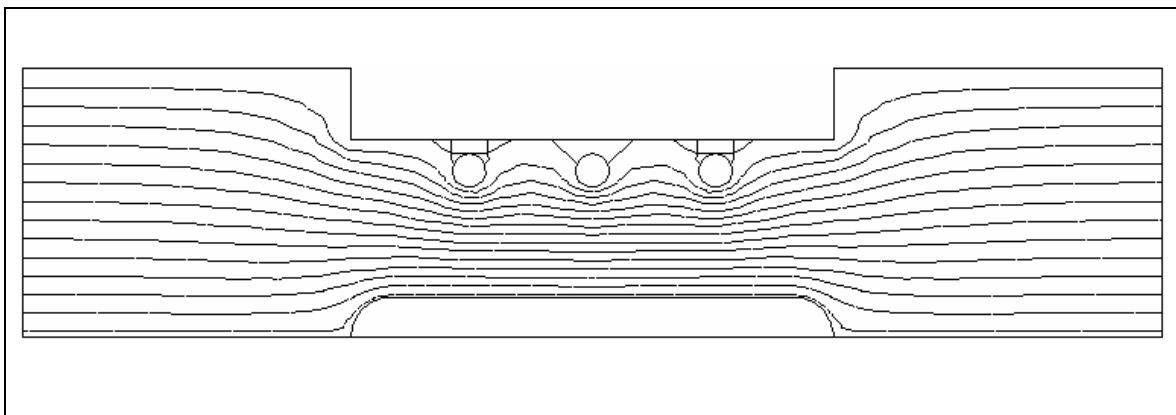


Figure 3.6:- D-Dot probe equipotential contours at intervals of 1 per-unit.

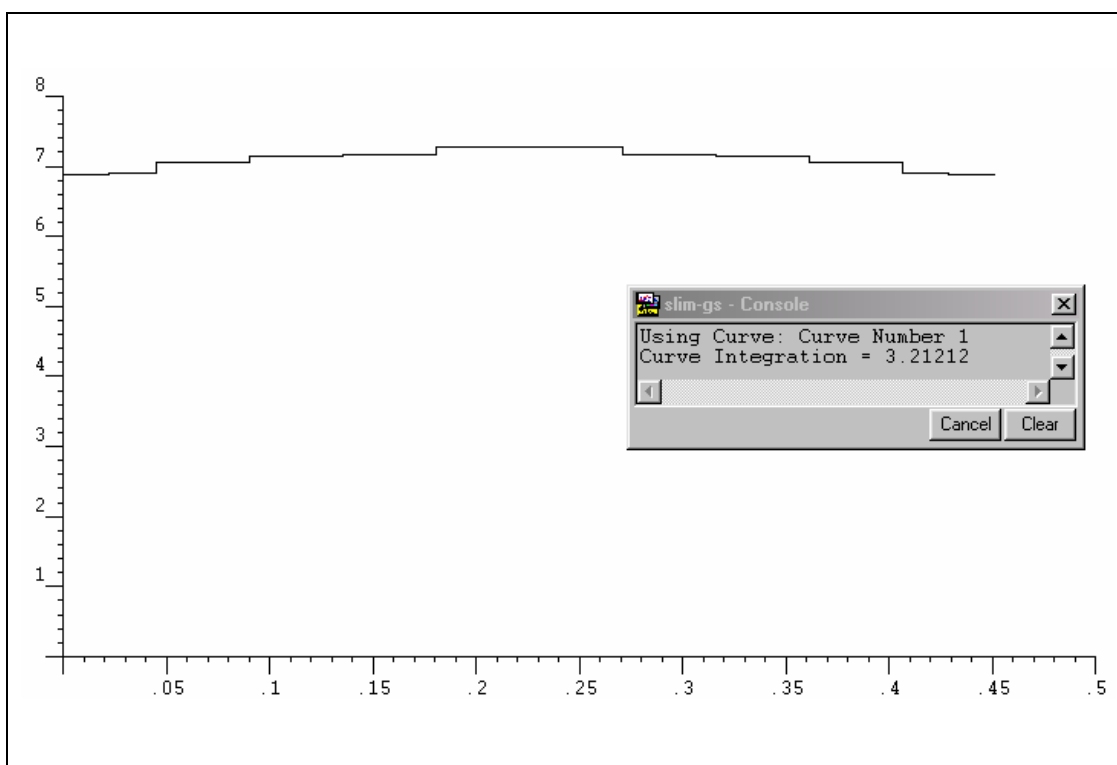


Figure 3.7:- Electric Field Along High Voltage Rod

With careful construction to eliminate any unnecessary roughness of the conductors surface and judicious profiling the maximum local field values predicted can be seen to be satisfactory.

### 3.4.3 Effect of Shielding/Field Modifying Toroids.

The effect of spacing between the signal toroid and the shielding/field modifying toroids was studied. It was found that with increased spacing the capacitance between the high voltage conductor and the signal toroid increases (Figure 3.15). However, increased spacing results in a decrease in the effectiveness of the shielding/field modifying toroids to prevent spurious signals being induced in the signal toroid. A compromise between the two criteria (maximum high voltage capacitance and maximum shielding) was chosen to be a spacing of 10cm between each shielding/field modifying toroids and the signal toroid.

### 3.4.4 Calculation of the Probe Ratio.

The groups of three similar toroids having minor/major-mean diameters of 38/405 mm respectively, are modeled. The group is axially arranged in a coaxial test rig. The middle toroid is fixed and electrically isolated from the main cylinder, while the other two toroids are movable up and down to control the value of  $C_2$  by changing the gap ( $\delta$ ) as shown in Figure 3.8. The axial high voltage rod has 45mm in radius while the inner diameter of the main cylinder is 422mm.

The value of the capacitance between the high voltage conductor and the signal toroid (at  $\delta = 100\text{mm}$ ) was calculated within the finite element program by applying unit potential to the signal toroid, and zero potential to the remaining toroids, high voltage conductor and outer shielding (Figure 3.12). Then by integrating the flux over the surface of the high voltage



conductor the capacitance between the signal toroid and high voltage conductor can be determined. The value of the high voltage arm capacitance was computed to be 3.63pF find from  $D \cdot 2\pi r L$  ( $2 \cdot 3.142 \cdot 0.045 \cdot 1.2856 \times 10^{-11}$ ), (Figure 3.13). Figure 3.13 to Figure 3.14 shows a spacing of 100mm between the signal toroid and the shielding/field modifying toroids. Figure 3.15 to Figure 3.16 shows a spacing of 210mm between the signal toroid and the shielding/field modifying toroids.

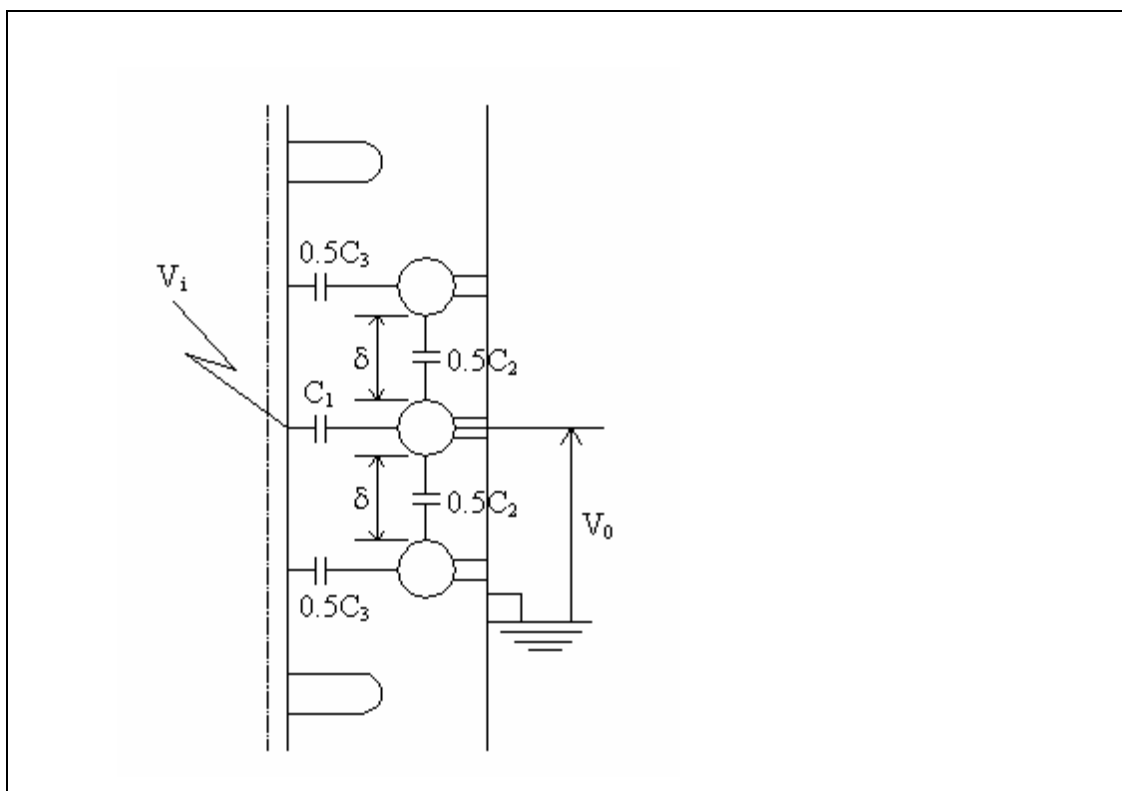
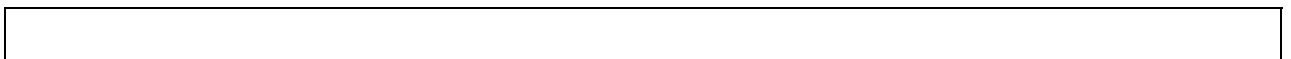


Figure 3.8:- Definition of the probe capacitances.



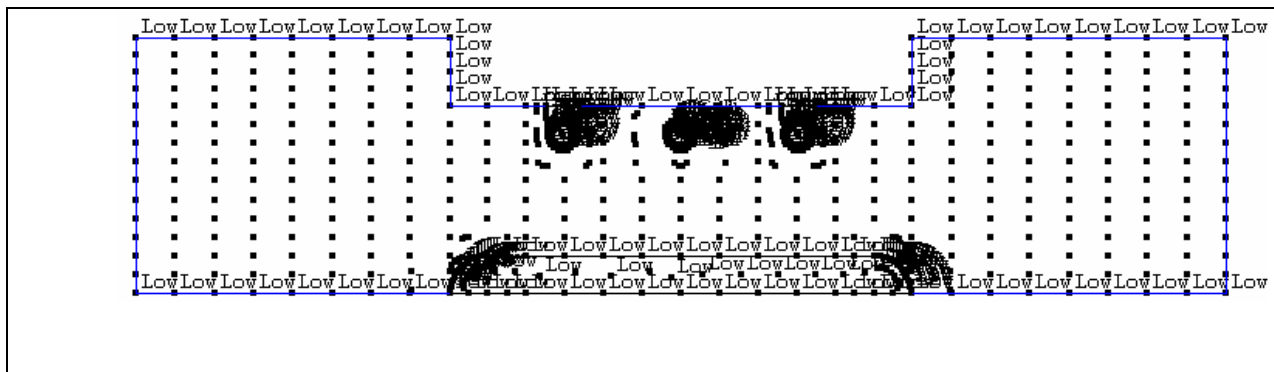


Figure 3.9:- 2D Mesh Generation

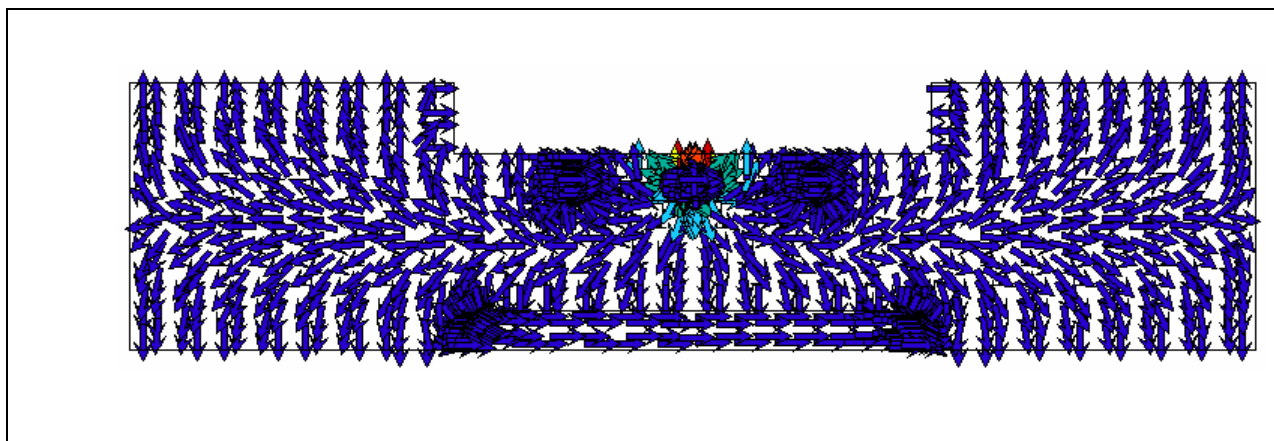


Figure 3.10:- Vector Display (Color Mode)

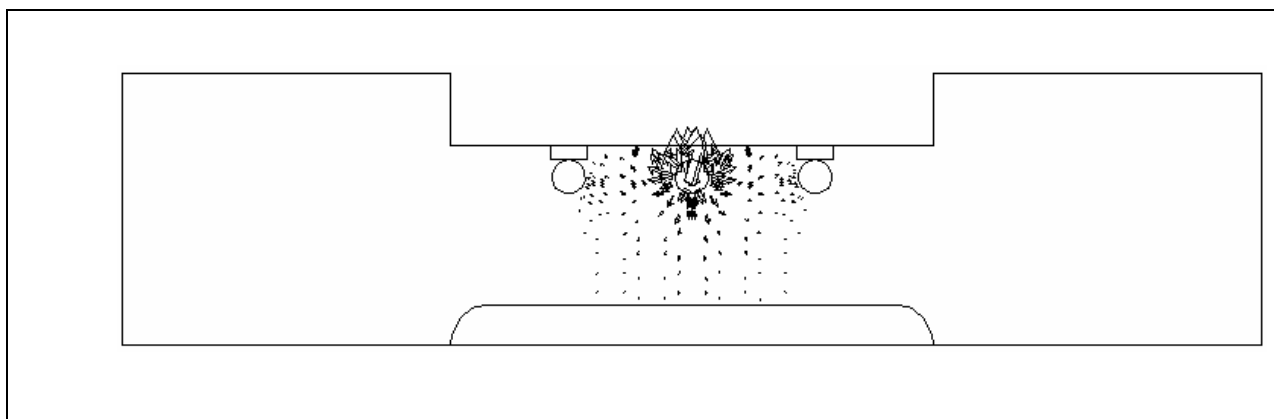
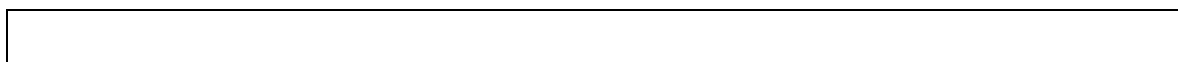


Figure 3.11:- Vector Display (Scaled Mode)



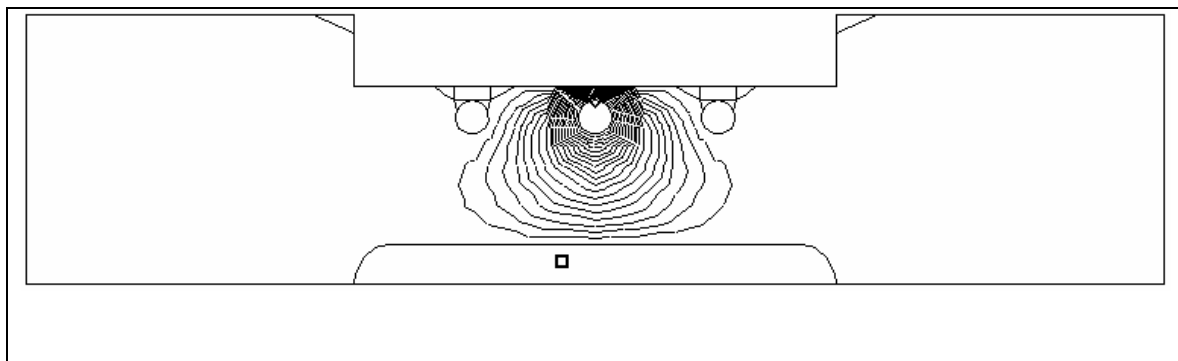


Figure 3.12:- D-Dot probe equipotential contours at intervals of 1 per-unit.

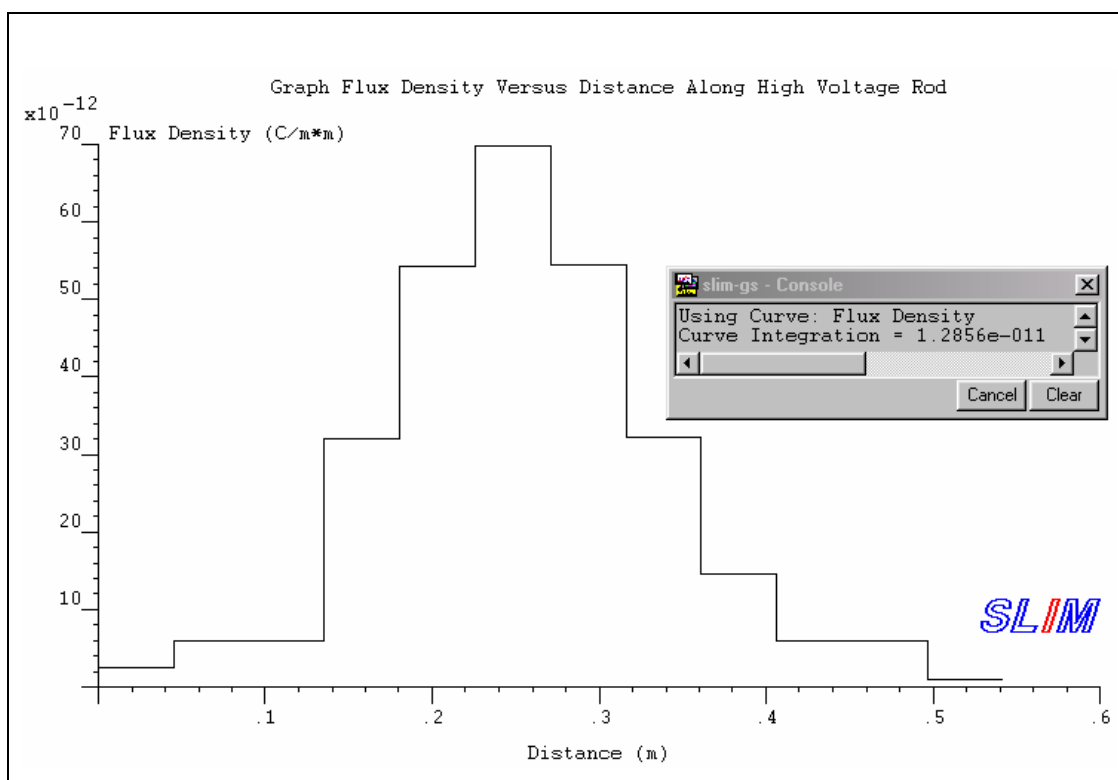
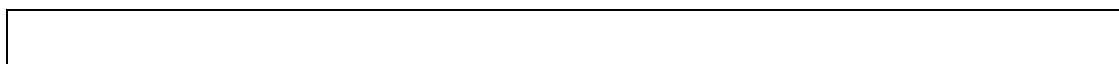


Figure 3.13:- Flux Density Over the Surface of The High Voltage Conductor



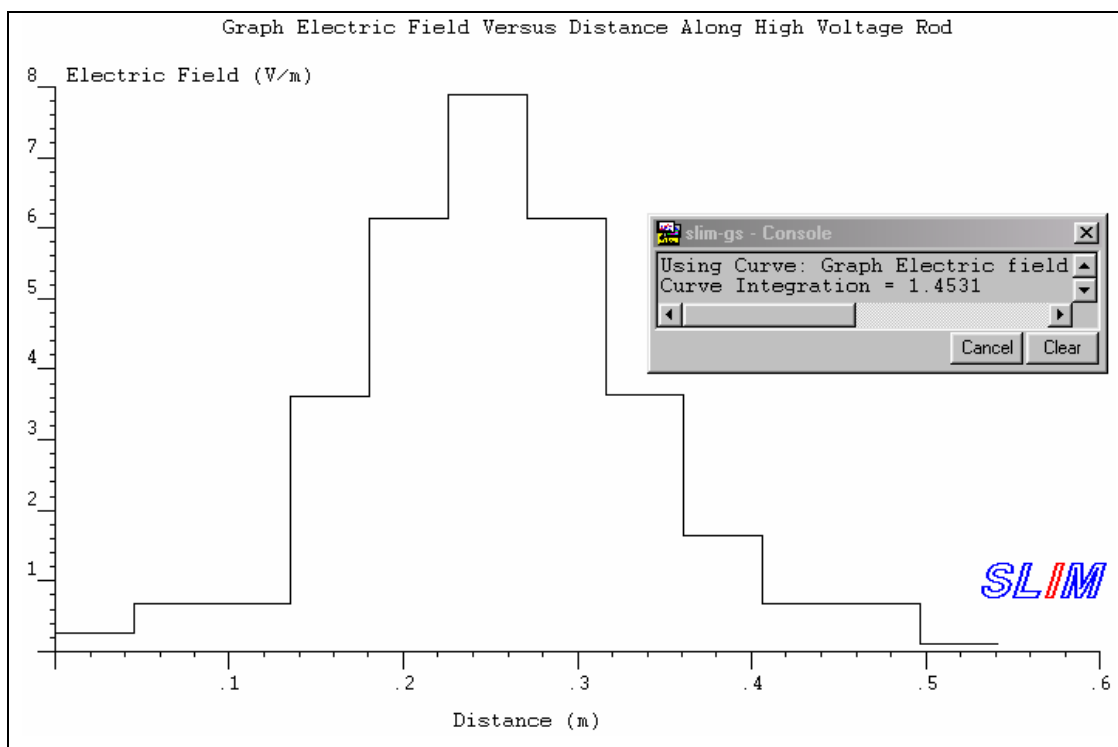


Figure 3.14:- Electric Field Over the Surface of The High Voltage Conductor

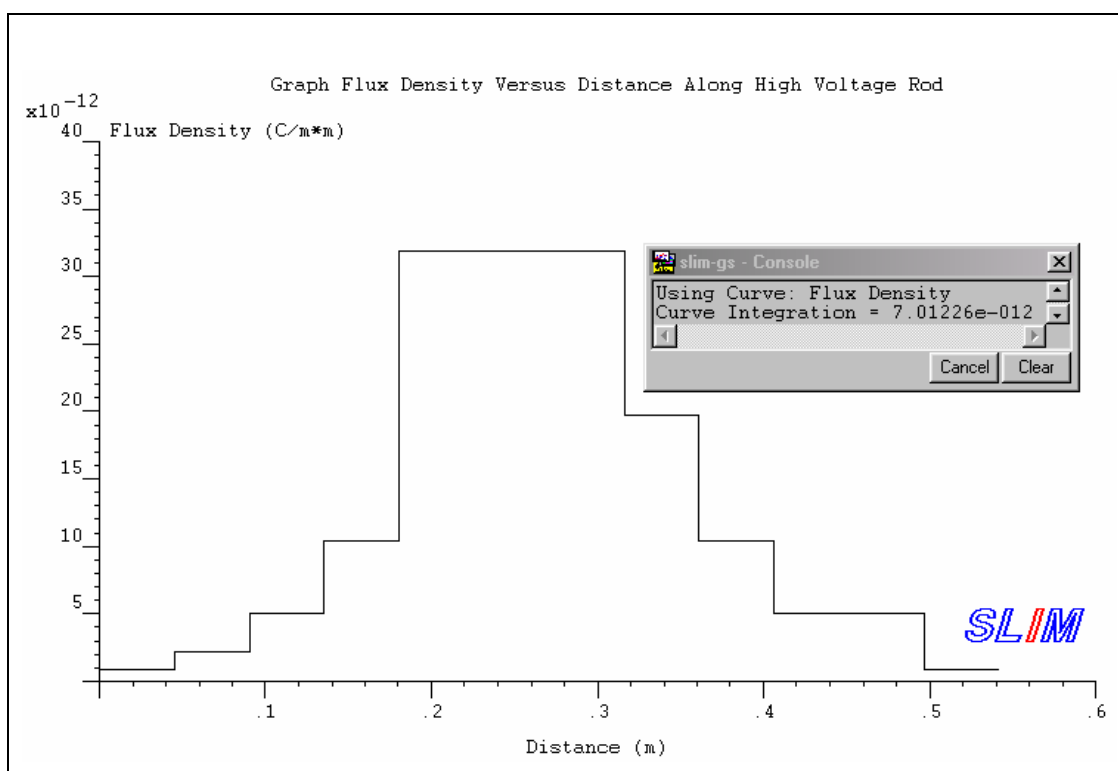
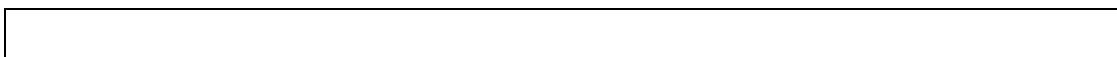


Figure 3.15:- Flux Density Over the Surface of The High Voltage Conductor



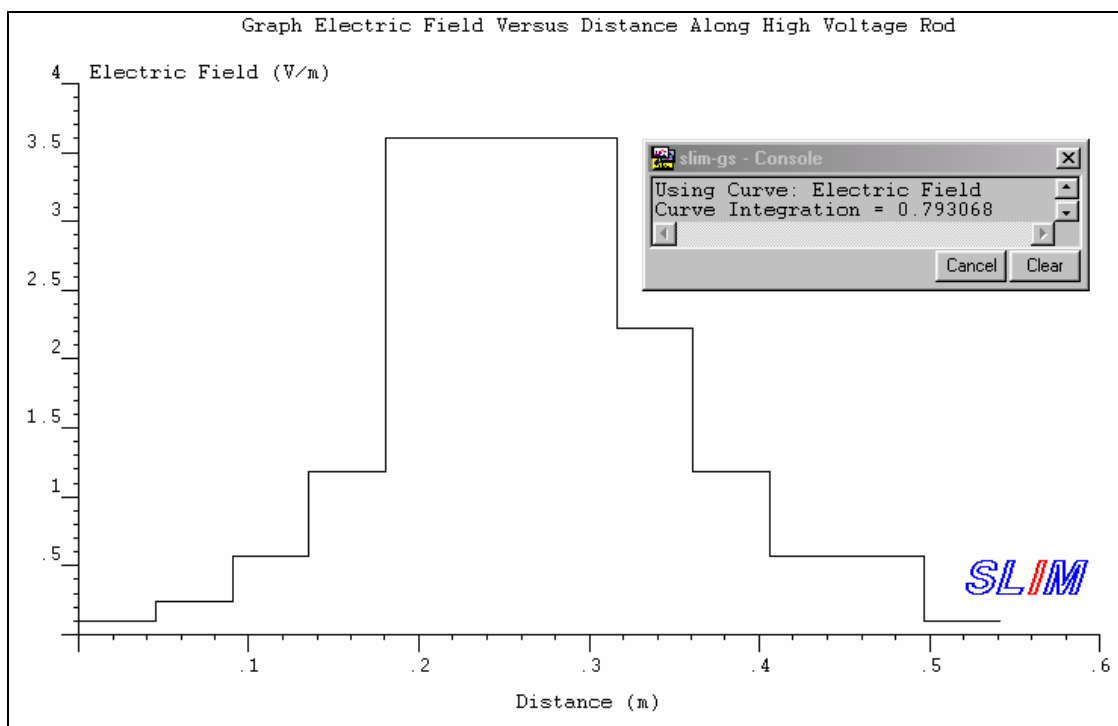


Figure 3.16:- Electric Field Over the Surface of The High Voltage Conductor

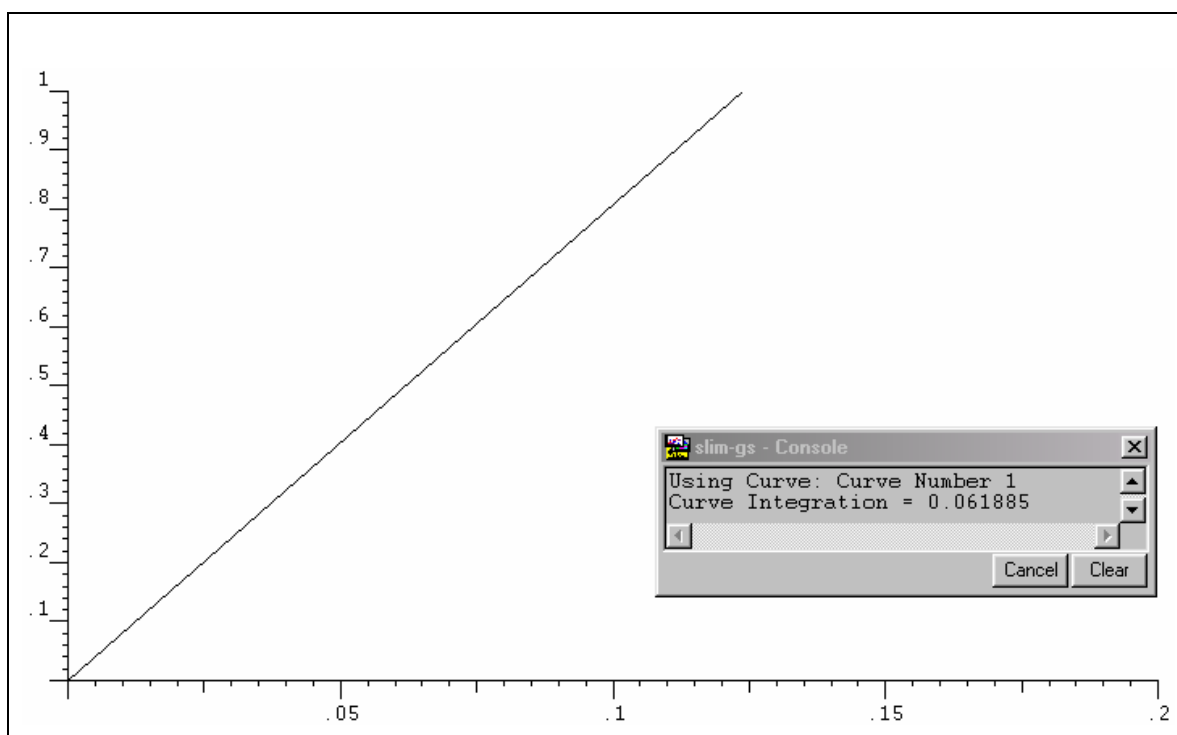


Figure 3.17:- Voltage Potential at Signal Toroid versus Distance

A low voltage arm comprising four 8.2nF high precision low-inductance capacitors connected in a radial manner together with a series damping resistor ( $5.5\Omega$ ) and a cable matching resistor ( $75\Omega$ ) is required to achieve a satisfactory output. Based on these values, the D-Dot probe divider ratio is then estimated as

$$\frac{V_H}{V_L} = \frac{C_L + C_H}{C_L} = \frac{3.63 \times 10^{-12} + (4 \times 8.2 \times 10^{-9})}{3.63 \times 10^{-12}} = 9.04 \times 10^3$$

The low-voltage arm is housed within an aluminium shielding enclosure. This is due to the fact that without the additional attenuator the capacitance of the signal cable would represent the bulk of the low-voltage arm capacitance is distributed nature then distorting the recorded output. The low-voltage attenuator along with the capacitance formed by the signal toroid forms the low-voltage arm capacitance. The capacitance of the triaxial cable is merely 2% of this attenuation capacitance.

## **CHAPTER IV**

### **D-DOT PROBE CONSTRUCTION**

#### **4.1 Materials**

##### **4.1.1 Aluminium**

Is an important commercial metal possessing some very unique properties. It is very light (density about 2.703) and some of its alloys are very strong, so its strength weight ratio makes its very attractive for aeronautical uses and other applications in which weight saving is important. Aluminium, especially in the pure form, has very high electrical and thermal conductivities, and is used as an electrical conductor in heat exchangers, etc. aluminium has good corrosion resistance, is nontoxic, and has a pleasing silvery white color; these properties make it attractive for applications in the food and container industry, architectural, and general structural fields.

Aluminium is very ductile and easily formed by casting and mechanical forming methods. Aluminium owes its good resistance to atmospheric corrosion to the formation of a tough, tenacious, highly insulating, thin oxide film, in spite of the fact that the metal itself is very anodic to other metals. In moist atmospheres, this protective oxide may not form, and some caution must be taken to maintain this film protection. Although aluminium can be joined by all welding processes, this same oxide film can interfere with the formation of good bonds during both fusion and resistance welding, and special fluxing and cleaning must accompany welding operations.

Pure aluminium melts at  $660^{\circ}\text{C}$  ( $1220\text{F}$ ). Aluminium has relatively high thermal and electrical conductivities. The metal is always covered with a thin, invisible film of oxide, which is impermeable and protective in character. Aluminium therefore, shows stability and long life under ordinary atmospheric exposure.

Exposure to atmospheres high in hydrogen sulfide or sulfur dioxide does not cause severe attack of aluminium at ordinary temperatures, and for this reason aluminium or its alloys can be used in atmospheres which could be rapidly corrosive to many other metals.

Aluminium parts should, as a rule, not be exposed to salt solutions while in electrical contact with copper, brass, nickel, tin, or steel parts, since galvanic attack of the aluminium is likely to occur. Contact with cadmium in such solutions results in no appreciable acceleration in attack on the aluminium, while contact with zinc (or-zinc-coated steel as long as the coating is intact) is generally beneficial, since the zinc is attacked selectively and cathodically protects adjacent areas of the aluminium.



Most organic acids and their water solutions have little or no effect on aluminium at room temperature, although oxalic acid is an exception and is corrosive. Concentrated nitric acid (about 80% by weight) and fuming sulfuric acid can be handled in aluminium containers. However, more dilute solutions of these acids are more active. All but the most dilute (less than 0.21%) solutions of hydrochloric and hydrofluoric acids have a rapid etching action on aluminium.

The outstanding characteristics of aluminium and its alloy are their strength-weight ratio, their resistance to corrosion, and their high thermal and electrical conductivity. The density of aluminium is about  $2770 \text{ kg/m}^3$  ( $0.10 \text{ lb/in}^3$ ), compared with  $7550 \text{ kg/m}^3$  ( $0.28 \text{ lb/in}^3$ ) for steel. Pure aluminium has a tensile strength of about  $90 \text{ MPa}$  ( $13 \text{ kpsi}$ ), but this can be improved considerably by cold working and also by alloying with other materials. The modulus of elasticity of aluminium, as well as of its alloys, is  $71 \text{ GPa}$  ( $10.3 \text{ Mpsi}$ ), which means that it has about one-third the stiffness of steel.

Solutions of the strong alkalies, potassium, or sodium hydroxides dissolve aluminium rapidly. However, ammonium hydroxide and many of the strong organic bases have little action on aluminium and are successfully used in contact with it.

Aluminium in the presence of water and limited air oxygen rapidly converts into aluminium hydroxide, a whitish powder [8].

## 4.2 Physical Structure

### 4.2.1 Coaxial Arrangement

Figure 3.3 shows the arrangement. The outer aluminium cylinder is 625mm high and has a diameter of 550mm. The D-Dot probe assembly comprises a signal toroid (1) and two similarly dimensioned shielding toroids (2) placed coaxially around the high voltage conductor. The whole probe assembly is contained within a cylindrical aluminium tube which has a diameter 422mm with stress toroid (5). The high voltage conductor is centered by an insulating spacer (Perspex). A low voltage arm (3) for the D-dot probe sensor is made radially connected capacitors and is contained within an aluminium shielding enclosure. The large aluminium cylinder, which encloses the transducers, provides electrostatic shielding in addition to providing a current return path to ground. The low voltage signals from the voltage transducers are transferred to the recording equipment via triaxial cables of approximately 28m in length. Connection from the high voltage conductor to the capacitor bank is made via the high pressure SF<sub>6</sub> spark gap which is pneumatically triggered.

### 4.2.2 Hollow (expand) Conductors.

Hollow conductors are used in high voltage conductor when, in order to reduce corona loss, it is desirable to increase the outside diameter without increasing the area beyond that needed for maximum economy. Not only is the initial corona voltage considerably higher than for conventional conductors of equal cross section, but the current carrying capacity for a given temperature rise is also greater because of the larger surface area available

for cooling and the better disposition of the metal with respect to skin effect when carrying alternating currents.

### **4.3 System Characteristic Parameters**

#### **4.3.1 Skin Effect**

Is a phenomenon, which occurs in conductors, carrying currents whose intensity varies rapidly from instant but does not occur with continuous currents. It arise from the fact that elements or filaments of variable current at different points in central or axial filament meets the maximum inductance, and in general the inductance offered to other filaments of current decreases as the distance of the filament from the axis tends to produce unequal current density over the cross section as a whole; the density is a minimum at the axis and a maximum at the periphery. Such distribution of the current density produces an increase in effective resistance and a decrease in effective internal inductance; the former is of more practical importance than the latter. In the case of large copper conductors at commercial power frequencies, and in the case of most conductors at carrier and radio frequencies, the increase in resistance should be considered.

#### **4.3.2 Corona Effect**

Corona is caused by the electric field next to an object exceeding the breakdown value for air (or whatever it is immersed in). Since the magnitude

of the field is inversely proportional to the radius of curvature, sharper edges break down sooner. The corona starting voltage is typically 30 kV/cm radius. Dust or water particles on the surface of the object reduce the corona starting voltage, probably by providing local areas of tighter curvature, and hence higher field stress.

The easiest case to analyze is that of a sphere. The magnitude of the electric field at the surface of a sphere in free space is simply the voltage/radius. Note that if the sphere is near another conductor, the field is no longer uniform, as the charge will redistribute itself towards an adjacent conductor, increasing the field.

Since corona is fundamentally a breakdown phenomenon, it follows Paschen's law: the voltage is a function of  $pd$ . Double all the dimensions and halve the gas pressure, and the corona voltage will be pretty much the same.

### 4.3.3 Conductor Losses

Conductor loss depends somewhat on frequency. This is because of an action called skin effect. When current flows through an isolated round wire, the magnetic flux associated with it is in the form of concentric circles. The flux density near the center of conductor is greater than it is near the surface. Consequently, the lines of flux near the center of the conductor encircle the inductance and causes the inductance near the center of the conductor to be greater than at the surface. Therefore, at radio frequencies, most of the current flows along the surface (outer skin) rather than near the center of the conductor. This is equivalent to reduce the cross sectional area of the conductor and increasing the opposition to current flow (that is, resistance). The additional opposition has a  $0^\circ$  phase angle and is, therefore

resistance and not a reactance. Therefore, the ac resistance of the conductor proportional to the square root of the frequency. The ratio of the ac resistance to the resistance of a conductor is called the resistance ratio. Above approximately 100MHz, the center of a conductor can be completely removed and have absolutely no effect on the total conductor loss.

#### **4.4 Complete Design**

##### **4.4.1 Materials for D-Dot Probe**

Table 1 gives the details of materials used.

##### **4.4.2 Engineering Drawing**

Figures 4.1 to 4.19 show all part and dimension of the D-dot probe. The construction and the arrangement of the probe was designed using the AutoCAD program. All dimensions are in millimeter (mm).

<b>Component Name</b>	<b>Materials</b>	<b>Quantity</b>
Aluminium Cylinder	Thin Pure Aluminium	2
Stress Modifying Toroids	Flexible Aluminium	2
Cylinder Spacer	Pure Aluminium (Solid)	8
Perspex Support	Perspex	2
Grounding Toroid	Pure Aluminium Toroid	2
Signal Toroid	Pure Aluminium Toroid	1
High Voltage Conductor (with screw threads)	Pure Aluminium (Hollow)	1
High Voltage End (Solid with screw threads)	Pure Aluminium (Solid)	1
High Voltage End (Solid)	Pure Aluminium (Solid)	1
Signal Toroid Spacer	Insulator (e.g. Perspex)	3
Attenuator	Pure Aluminium (Body). Insulator (Between Signal Conductor & Grounding Body)	1
Grounding Toroid Spacer	Pure Aluminium (Solid)	8

Table 4.1 Materials used for D-dot Probe Assembly

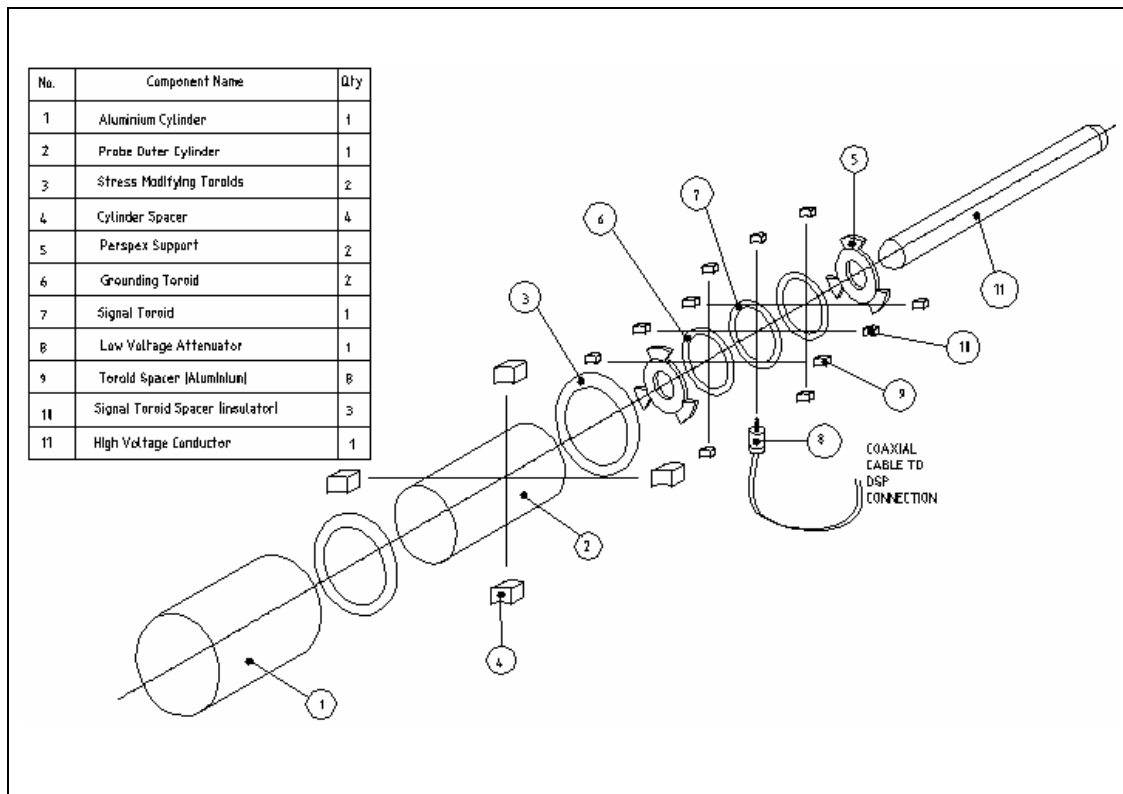


Figure 4.1 Component in the D-dot Probe

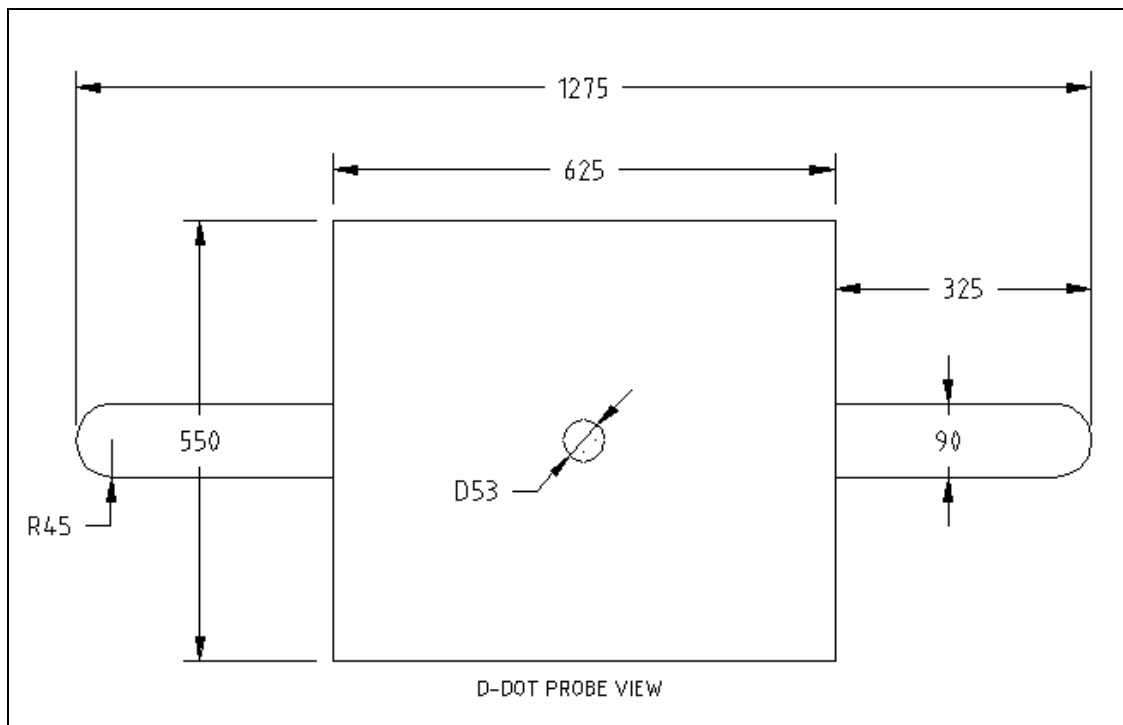
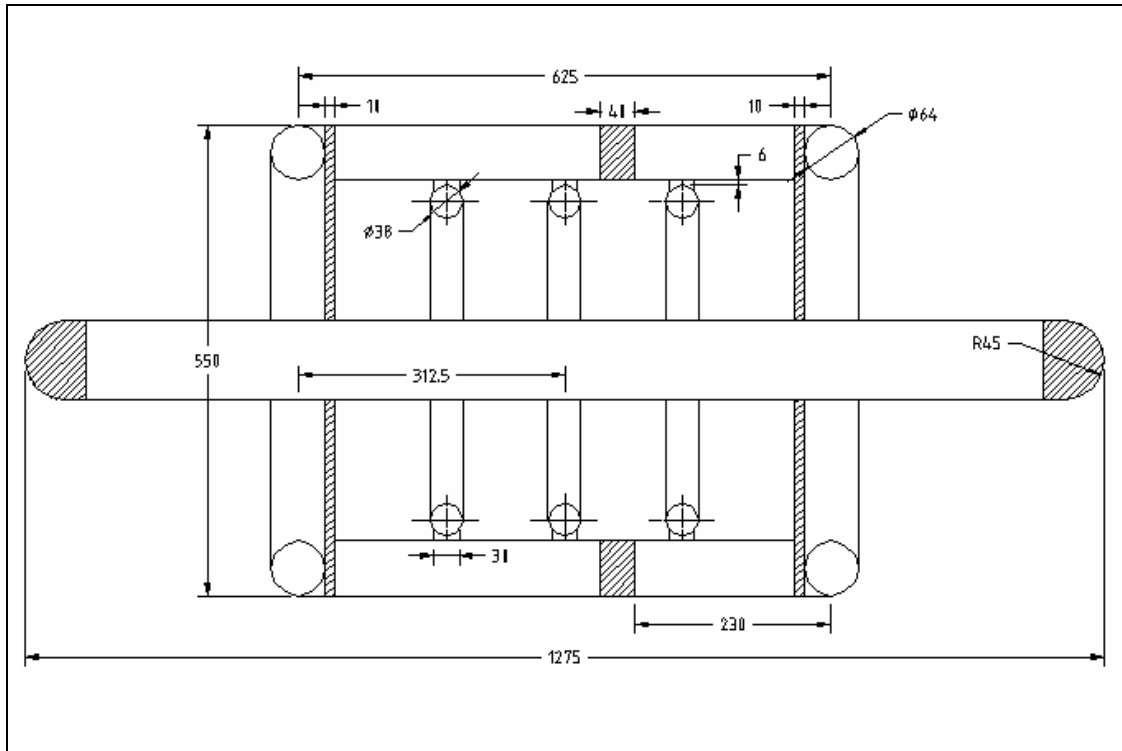
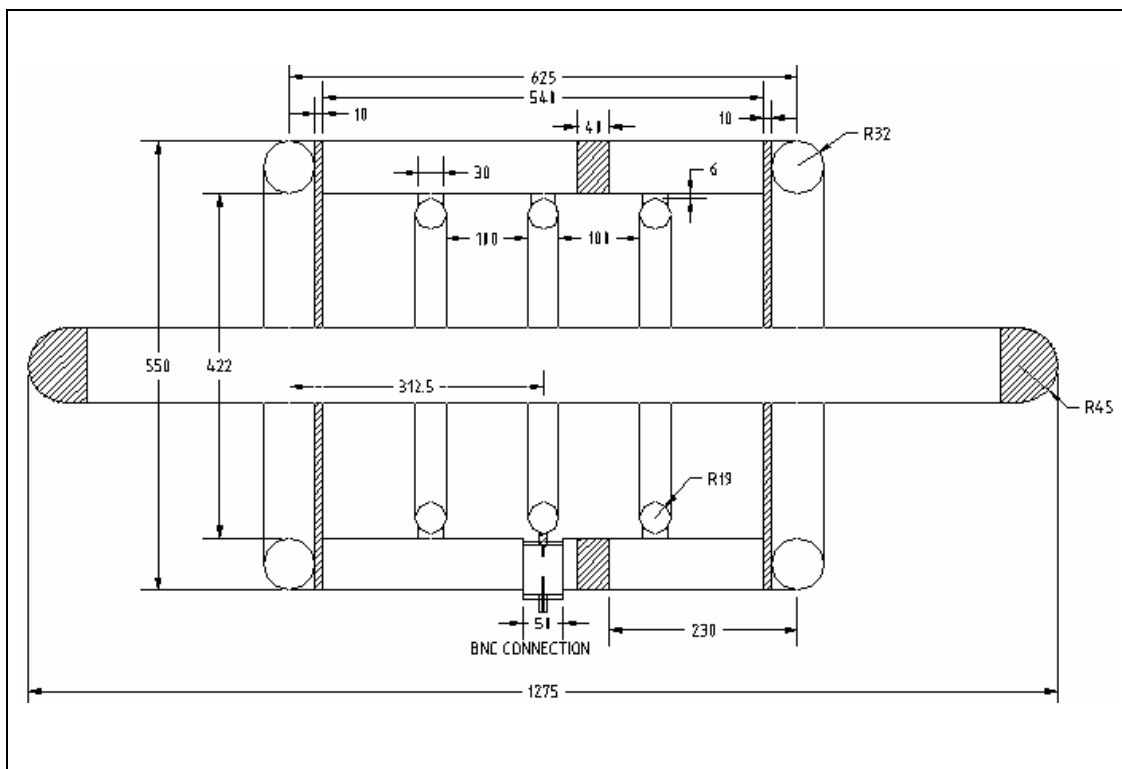


Figure 4.2 D-dot probe view from one side



**Figure 4.3 Dimension of D-dot probe (slice at the middle)**



**Figure 4.4 Dimension of D-dot probe with attenuator**



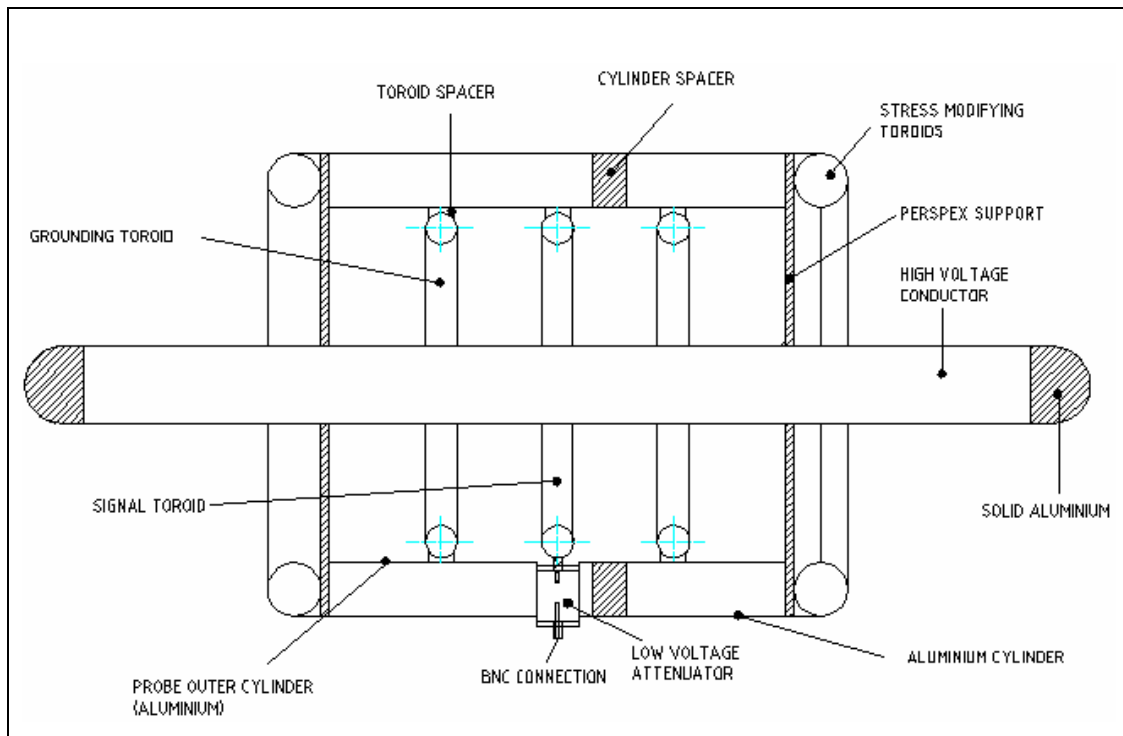


**Figure 4.5 Schematic diagram of D-dot probe arrangement.**

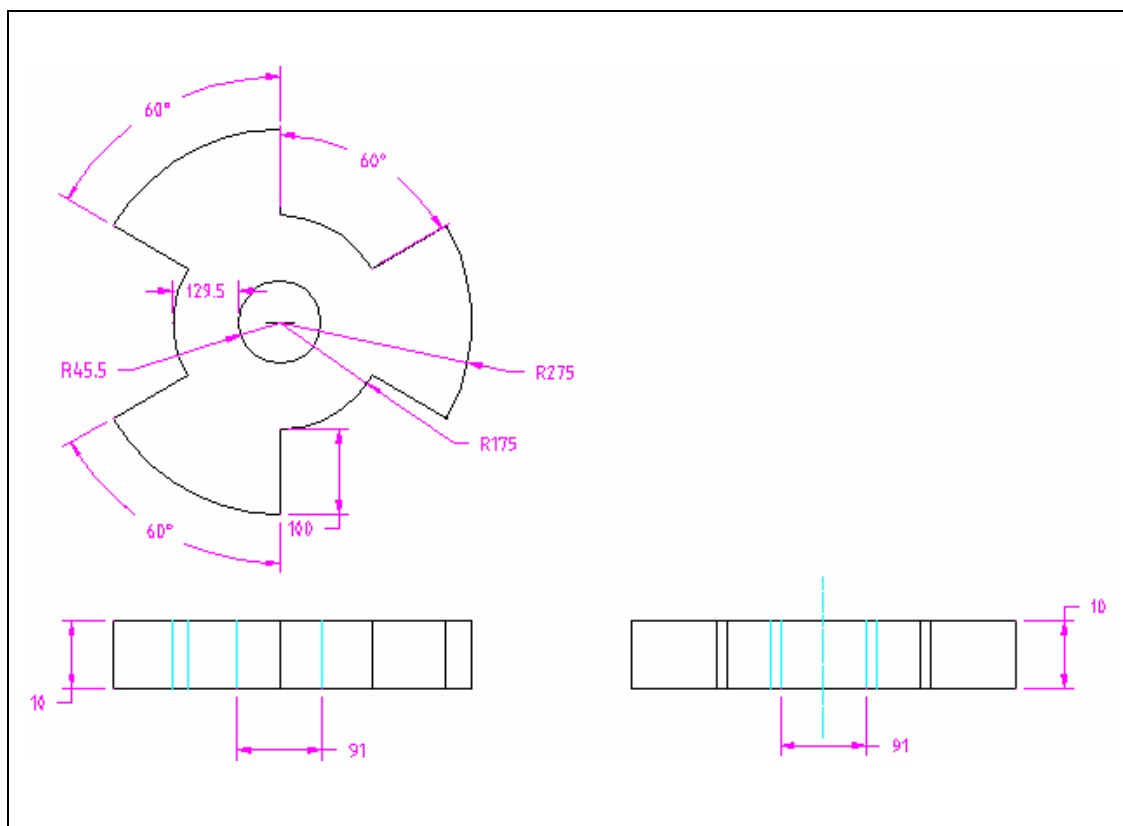


**Figure 4.6 Perspex support for high voltage rod**

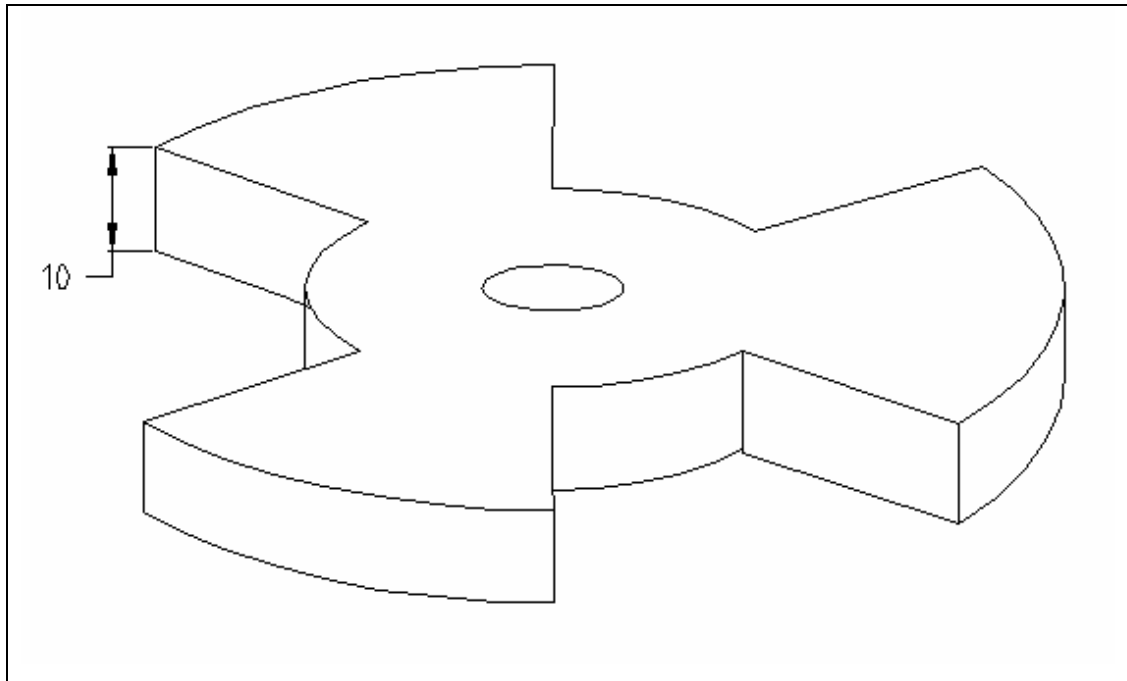


**Figure 4.7 Perspex support for high voltage rod (3 D view)**

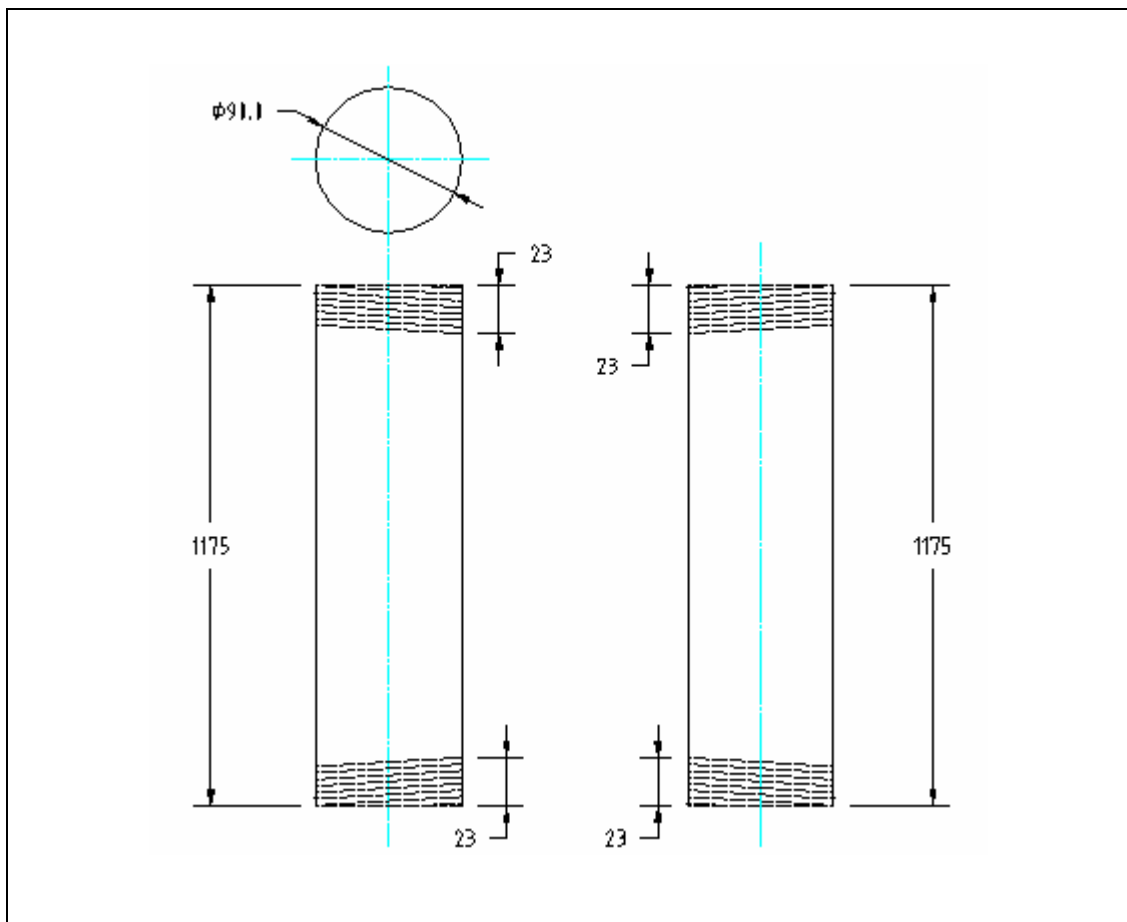


**Figure 4.8 High voltage rod without ending screw**

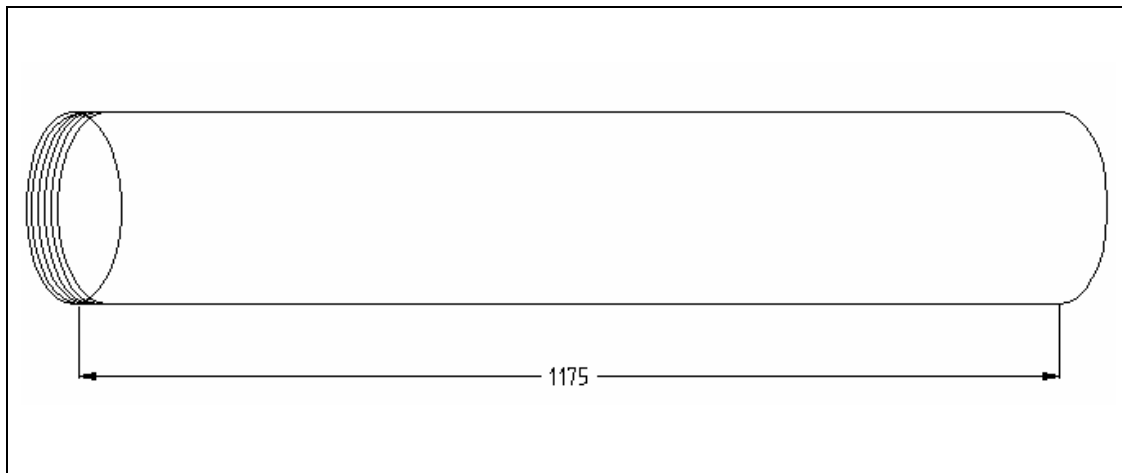


**Figure 4.9 High voltage rod without ending screw (3 D view)**

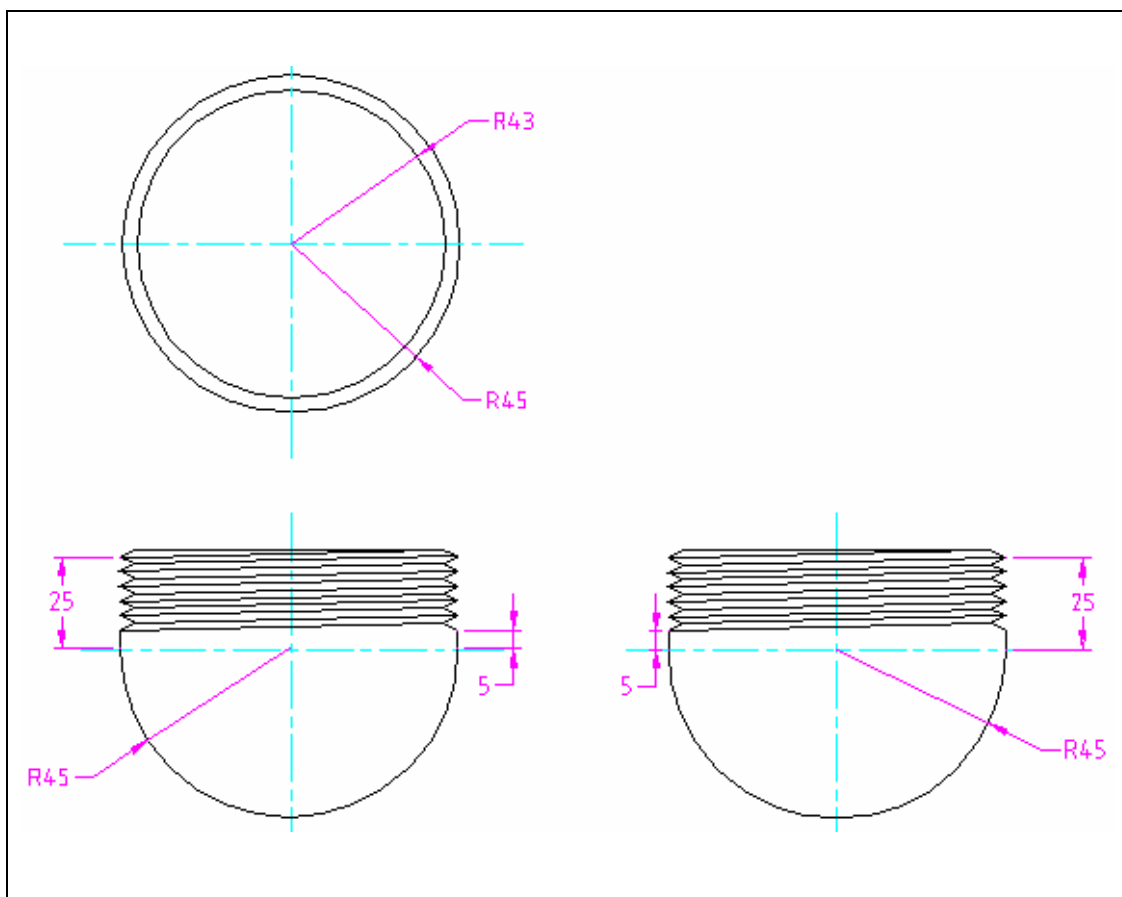


**Figure 4.10 Solid ending screw for high voltage rod**

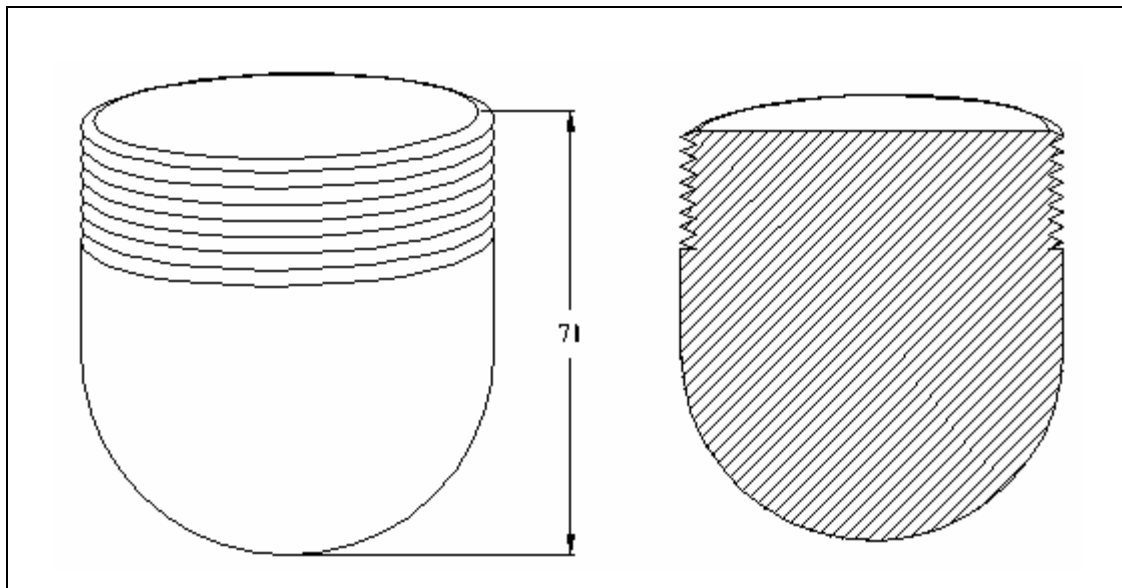


**Figure 4.11 Solid ending screw for high voltage rod (3 D view)**

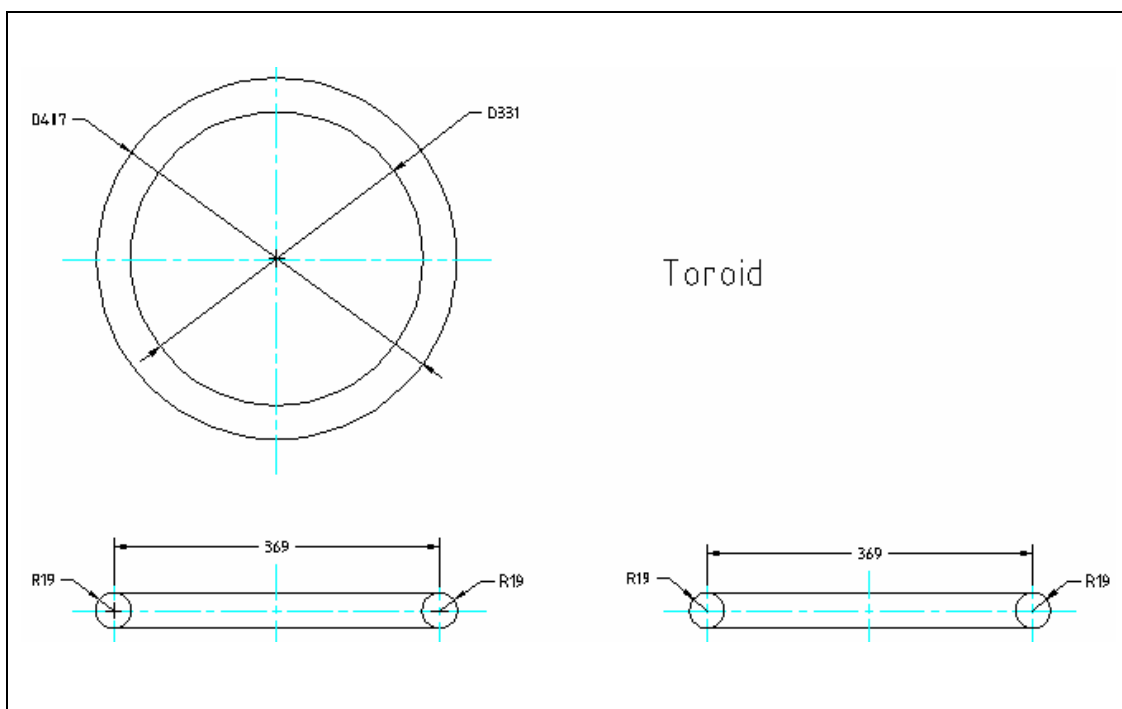


**Figure 4.12 Signal and grounding toroids**

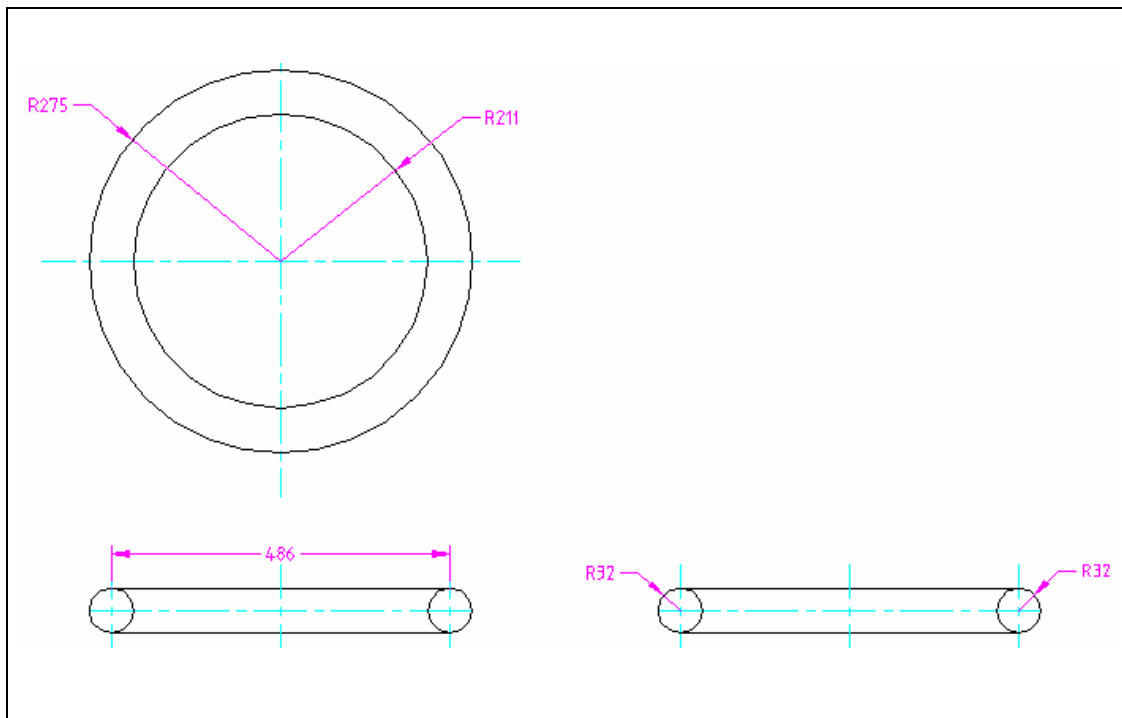


Figure 4.13 Stress modifying toroids

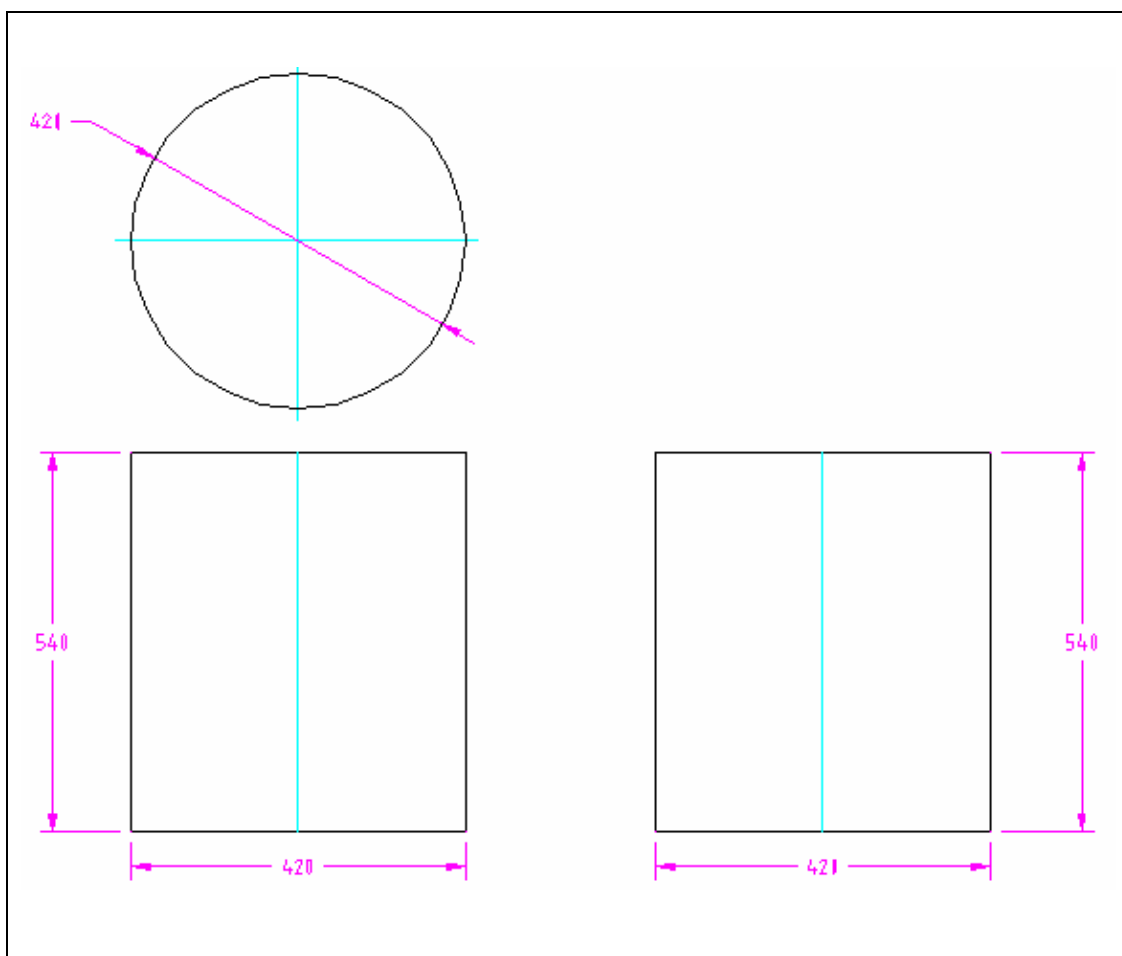
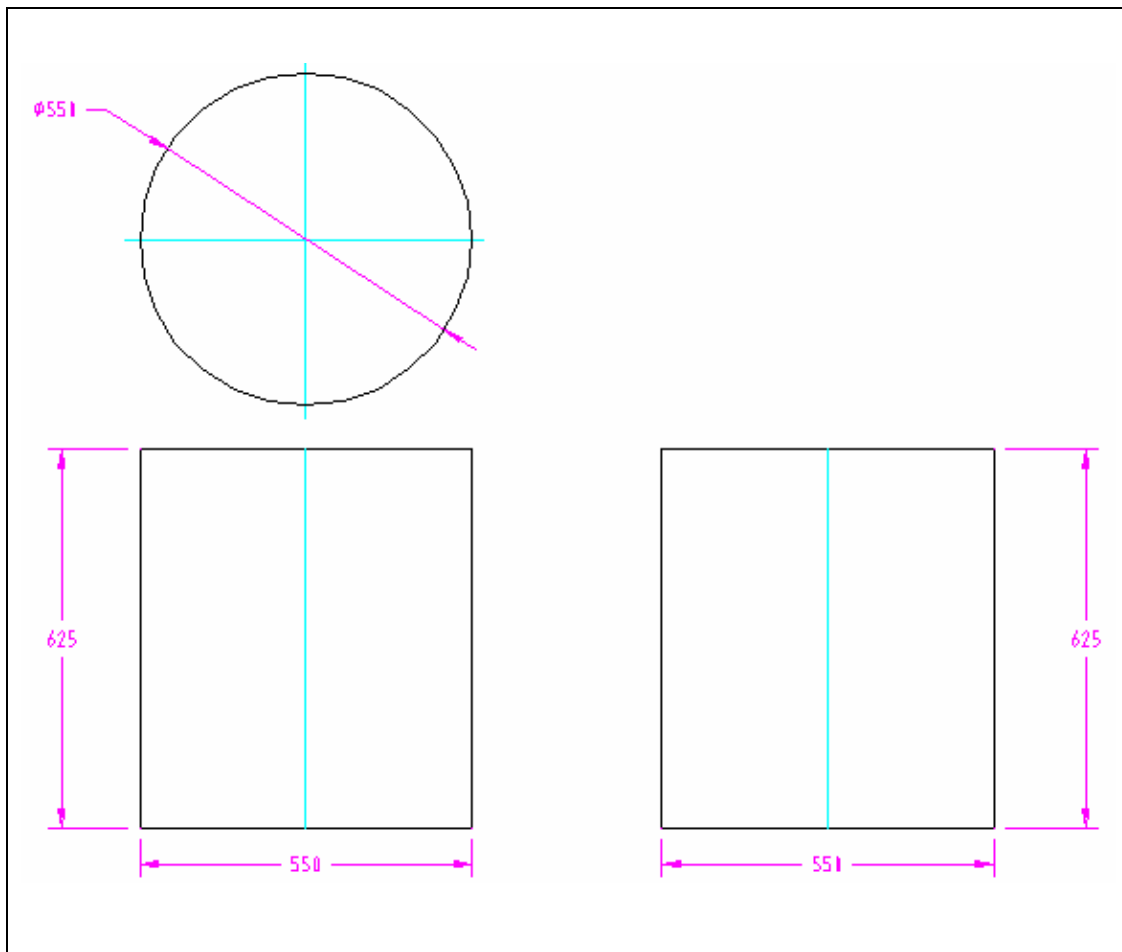


Figure 4.14 Thin cylinder aluminium (inner)



**Figure 4.15 Thin cylinder aluminium (outer)**

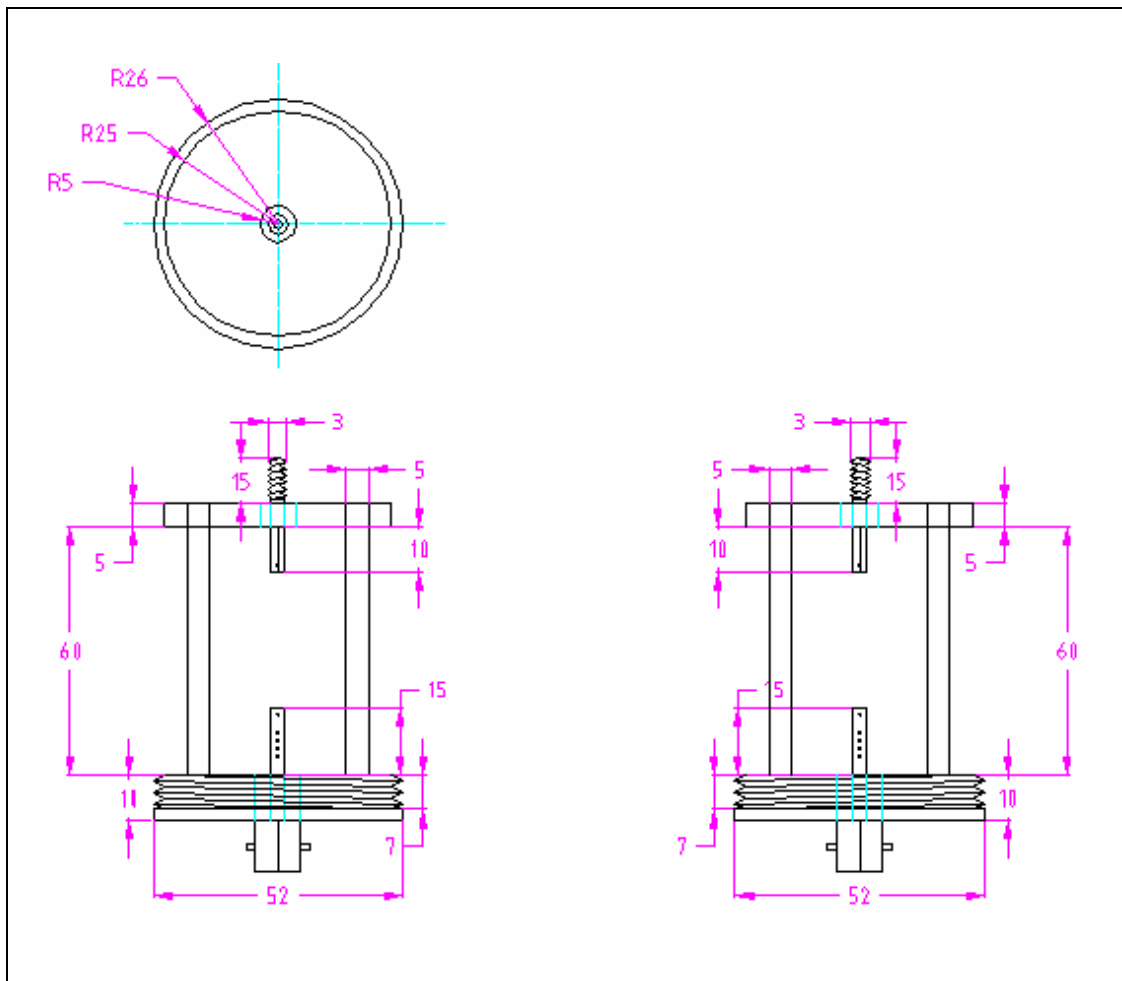


Figure 4.16 Attenuator

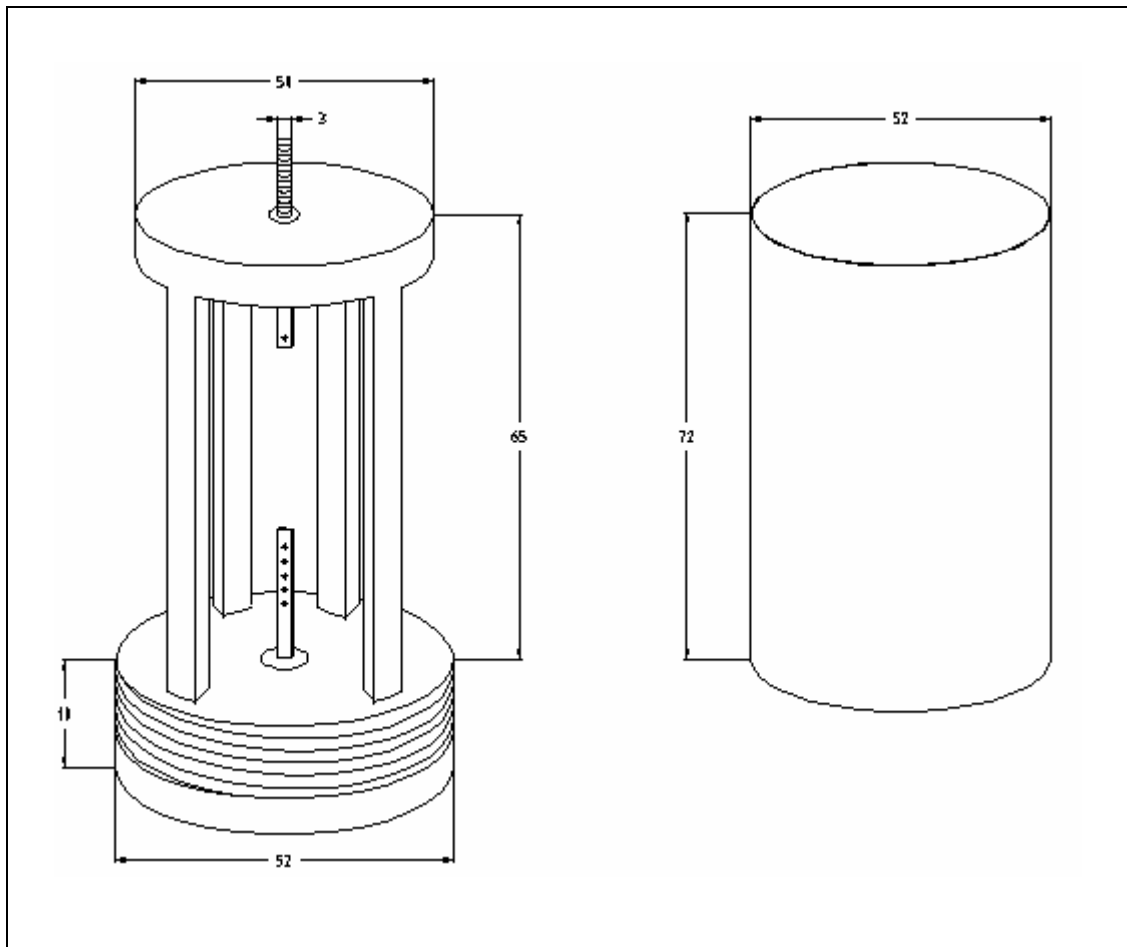
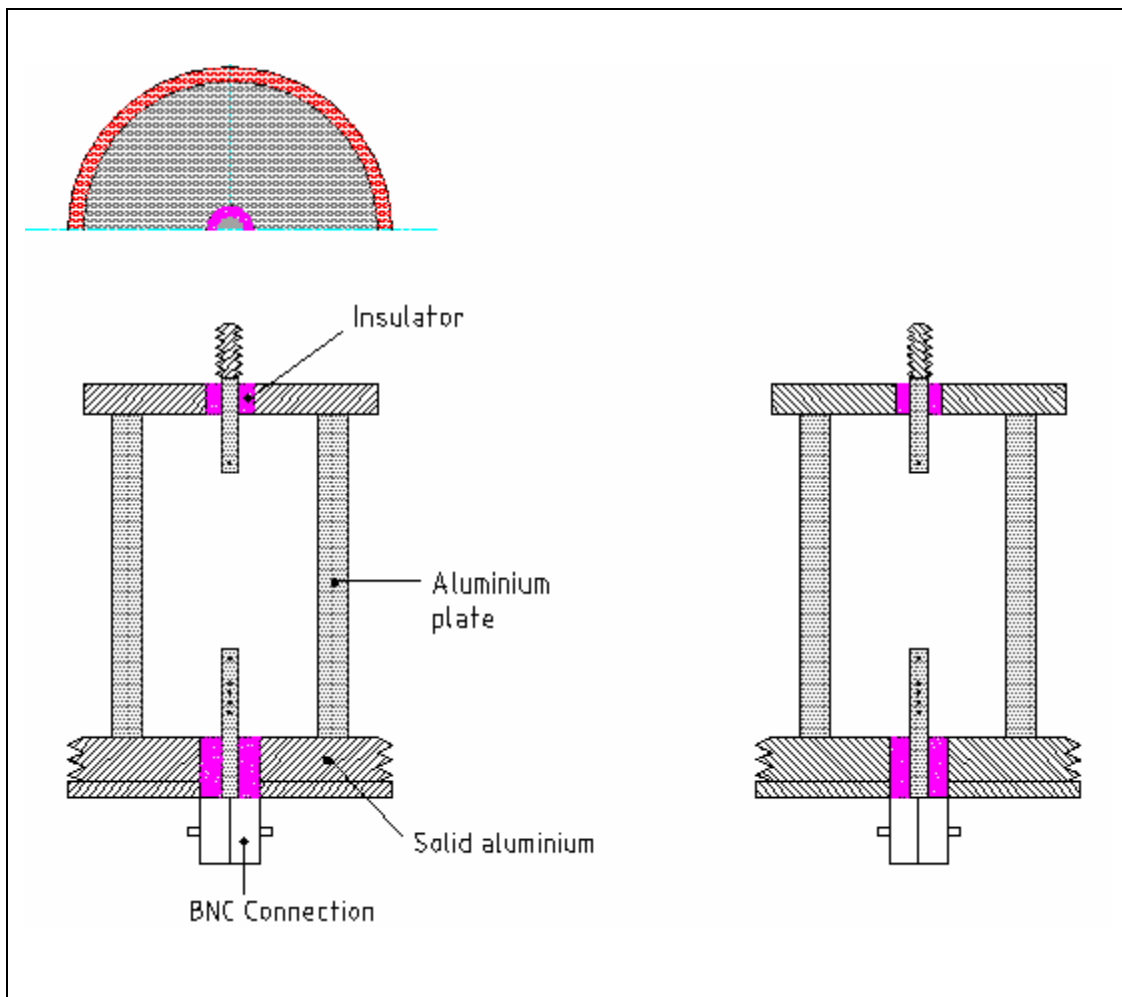
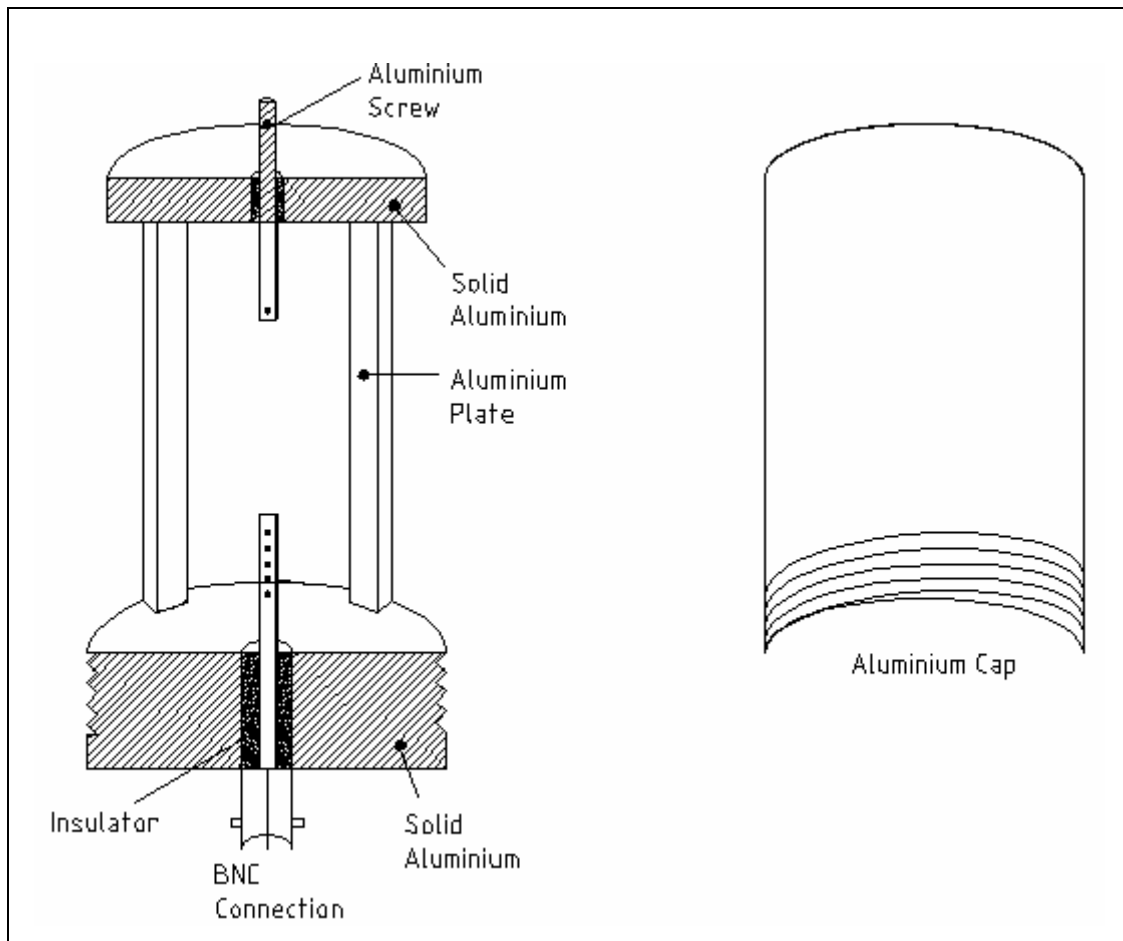


Figure 4.17 Attenuator (3 D view)





**Figure 4.18 Attenuator schematic arrangement**



**Figure 4.19 Attenuator arrangement**

## **CHAPTER V**

### **CONCLUSIONS AND SUGGESTIONS**

#### **5.1 Discussion**

Within this project, there is a strong tendency to support "electrical field measurements" performed by the D-Dot probe, instead of "voltage measurements" as performed by voltage dividers. By comparing some results of simultaneous measurements for impulse voltage transients made on different kinds of HV equipment it is apparently demonstrated that such electrical field measurements can significantly improve this difficult and specialized measurement technique. However, it is afraid that this tendency can be misunderstood and thus it is necessary to draw attention to the following fundamental statements.

Due to the very well-known theory and practice of impulse voltage dividers, the development of which has quite a long history, the limitations concerned with the voltage transfer characteristics of such dividers are well known. The most advanced theory of voltage dividers is based upon traveling wave or transmission line theory, i.e., by taking the propagation of electromagnetic waves in one dimension into account. It should also be well

known that this theory has a fundamental limitation for proper application in the definition of an input voltage of any transmission system that is simulated by this theory. This input voltage can be defined by the condition that an electrostatic field exists for which  $\oint_c E \cdot ds = 0$ , within a plane of limited extension in both directions. This condition, however, is not fulfilled for all high voltage impulse measurements, for which the distance between two points of different potentials  $V$ , i.e., between an HV terminal of any piece of equipment and ground potential, becomes larger than some fraction of the wavelength,  $\lambda$ , of the transient voltage, assumed to be sinusoidal or harmonic, with frequency  $f = 1/\lambda$ . A quite optimistic interpretation of "some fraction" would be a factor of 1/10 and assuming that the electrical field is built up within a plane or space, for which vacuum conditions can be assumed ( $\epsilon = \epsilon_0$ ,  $\mu = \mu_0$ ) the velocity of light,  $c_0$ , will govern the most optimistic assumption for electrostatic conditions, for which the definition of any voltage, i.e., the difference of potentials, is still possible. If, therefore, a voltage pulse to be measured between terminals being separated by some distance  $d$  contains frequencies  $f_u$  higher than about  $c_0(10d)^{-1}$ , the definition of a "voltage" becomes questionable. Note that even a distance of only 1 m restricts  $f_u$  to 30 MHz.

At this point one should consider that the most difficult problems concerned with voltage dividers, i.e., the problems related to the connection between voltage divider and terminals of test objects ('lead to divider'), or the bandwidth of the best possible divider structures, can be related to this fundamental problem. But as far as the application of voltage dividers is concerned, it is quite possible to achieve a bandwidth  $f_B$  which may well be in agreement with the above-mentioned limitations, if the dividers are carefully built and constructed. This was demonstrated by calculations as well as by measurements in the original publication concerned with "damped capacitive voltage divider" There it was shown that  $f_B$  can be as high about  $f_B \approx (2h\sqrt{L'C'_e})^{-1}$ , where  $L'$  is the inductance per unit length (p.u.l.),  $C'_e$  is its stray capacitance p.u.l. to ground, and  $h$  is the height or length of the divider column. It is unnecessary to show that this expression is related to the travel

time of the voltage transient necessary to reach ground potential. This high bandwidth can, of course, only be reached by an optimal design of the dividers.

Nevertheless, the application of field sensing device as has been done at ground or at HV potential for a long time is certainly a good tool to supplement high voltage impulse measurements, if it is done with care.

## 5.2 Conclusions

In most test-applications the full impulse voltage is a lightning or a switching impulse voltage. These impulse voltages can be measured quite accurate with voltage dividers. The present work has been directed towards the developments of a better understanding of the transient response measurements. Method for improved impulse voltage measurement techniques have been described and compared to the conventional voltage divider method. The techniques is based upon the D-dot probe principle used in pulse-power applications. Its design and capacitance for voltage ratio determination has been derived from electric field computations. The D-dot probe has been designed as a portable unit enabling it to be incorporated in any suitable system.

According to the experimental results obtained from Naylor P [9], the method demonstrate unequivocally that there is no evidence of a voltage overshoot/spike on the front of the residual voltage waveform. Such observations can still be made even when the rate-of-rise of voltage at the arrester terminals is in the order of 1 kV/ns. The rate-of-rise, is comparable to those that can be anticipated for an unattenuated lightning strike close to the arrester terminals. Such overshoots that have been reported in the literature may be ascribed with the voltage divider measurements.

From the results in Chapter 3, charge simulation modeling by SLIM analysis gives the capacitive equivalent circuit and the best arrangement of the probe. Good linear calibration curve is obtained for the probe against the conventional capacitive divider. Also faster response and less inductive overshoot are achieved from the calibration of the D-dot probe.

It can be concluded that the D-dot probe based sensor will improve the impulse voltage measurement. The high accuracy necessary for the measurement of an amplitude of an impulse voltage will be performed with voltage dividers, but the waveshape of the impulse voltage will additionally be evaluated from measuring systems, like the D-dot probe based sensor.

### **5.3 Suggestions**

The constructed D-Dot probe based divider need to be tested and calibrated against a standard divider. It is suggested that this is done in the next phase of the research where a complete test system consisting the high current generator, surge arrester load and the transducer are assembled. The performance of the D-Dor probe based sensor can therefore be ascertained.

## REFERENCES

- [1] Schwab, A.J. (1972): "High Voltage Measurement Technique" M.I.T. Press, Cambridge, Massachusetts.
- [2] Haddad, A., Naylor, P., Metwally, I.A., German, D.M. and Waters, R.T. (1995): "An Improved Non Inductive Impulse Voltage Measurement Technique for ZnO Surge Arresters" IEEE Transactions on Power Delivery, Vol. 10, No. 2, pp. 778-785.
- [3] Barker, P.P., Mancao, R.T., Kvalfine, D.J. and Parrish, D.E. (1993). "Characteristic of Lightning Surges Measured at Metal Oxide Distribution Arresters." IEEE Transactions on Power delivery, Vol.8, No. 1, pp.301-310.
- [4] Feser, K., PtA W., Weyreter, G., Gockenbach, E. (July 1988). "Distortion Free Measurement Of High Impulse Voltages." IEEE Transactions on Power Delivery, Volume 3, No. 3.
- [5] Van Heesch, E.J.M., Van Deursen, A.P.J., Van Houten, M.A., Jacobs, G.A.P., Kersten, W.F.J. and Van Der Laan, P.C.T. (1989). "Field Tests and Response of The D/I H.V. Measuring System." Sixth International

Symposium on High Voltage Engineering, New Orleans (USA), Vol. 3,  
Paper 42.23.

- [6] Rifijin, L., Caixin, S. and Xiaoguang, Z. (1993). "Development of A Transient Voltage Measuring System." Eight International Symposium on High Voltage Engineering, Yokohama (Japan), Vol. 4, Paper 54.16, pp. 141144.
  
- [7] Van Deursen, A.P.J., Gulickx, P.F.M. and Van der Laan, P.C.T. (1993). "A Current and Voltage Sensor Combined in One Unit." Eight International Symposium on High Voltage Engineering, Yokohama (Japan), Vol. 2, Paper 56.027 pp. 463-466.
  
- [8] Brody & Clause. (1986). -Material Handbook." 12~h Ed. McGrawhill Book Company.
  
- [9] Naylor, P. (1995). "The Transient Response of High-Voltage Surge Arresters" PhD Thesis, University of Wales, Cardiff (UK).
  
- [10] Kind, D. (1978). "An Introduction To High-Voltage Experimental Technique" Vieweg & Sohn Verlagsgesellschaft mbH, Braunschweig.
  
- [11] Naidu, M.S. and Kamaraju, V. (1995). "High Voltage Engineering" McGraw-Hill, New York.



- [12] Gallagher, T.J. and Pearmain, A.J. (1983). "High Voltage Measurement, Testing and Design." John Wiley & Sons, Chichester.
- [13] Kuffel, E. and Zaengl, W.S. (1984). "High Voltage Engineering Fundamentals" Pergamon Press, New York.
- [14] Khalifa, M. (1990). "High Voltage Engineering Theory and Practice" Marcel Dekker Inc, New York.
- [15] Metwally, I.A. (1985). "-Coaxial D-Dot Probe: Design and Testing" Electrical Insulation and Dielectric Phenomena, Annual Report, Mansoura University, Egypt, pp. 298-301.
- [16] Haddad, A., Naylor, P., German, D.M., Waters, R.T. (1995). "A Low Inductance 60kV Test Module for Distribution Surge Arresters" Ninth International Symposium on High Voltage Engineering, Graz (Austria), Paper No. 4559.
- [17] Z. Abdul-Malek. (1999). "Fast Transient Response of High-Voltage Surge Arresters" PhD Thesis, University of Wales, Cardiff (UK).
- [18] Z. Abdul-Malek. (1995). "Lightning Impulse Test on High Voltage Surge Arresters" Master Thesis, University of Wales, Cardiff (UK).

- [19] Bowdler, G.W. (1973). "Measurement in High Voltage Test Circuits"  
Pergamon Press, Oxford.
  
- [20] Skitek, G.G., Marshall, S.V. (1990). "Electromagnetic Concepts and  
Applications" 3rd Edition, Prentice Hall.
  
- [21] Ryan, H.M. (1994). "High Voltage Engineering and Testing" Peter  
Peregrinus Ltd, London.
  
- [22] Kuffel, E. and Abdullah, M. (1970). "High Voltage Engineering"  
Pergamon Press, New York.
  
- [23] ASTM, ASTM D3426-97. "Standard Test Method for Dielectric  
Breakdown Voltage and Dielectric Strength of Solid Electrical Insulating  
Materials Using Impulse Waves" (1988).